

Repeatability Study of the Dynamic Rollover Test System (DRoTS) Using an Objective Rating Method

A Thesis

Presented to

the faculty of the School of Engineering and Applied Science

University of Virginia

In Partial Fulfillment

of the Requirements for the Degree

Master of Science

Mechanical and Aerospace Engineering

by:

Jeremy Hansen Seppi

May, 2015

APPROVAL SHEET

The thesis

is submitted in partial fulfillment of the requirements for the degree of

Master of Science

Mechanical and Aerospace Engineering



Jeremy Hansen. Seppi, Author

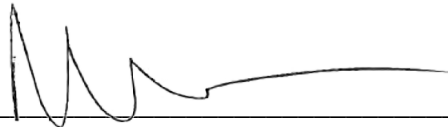
The thesis has been read and approved by the examining committee:



Jeff R. Crandall, Thesis Advisor

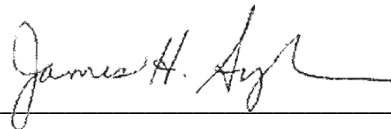


Richard W. Kent, Committee Chair



Mark R. Sochor, Committee Member

Accepted for the School of Engineering and Applied Science:



Dean, School of Engineering and Applied Science

May 2015

ABSTRACT

The combination of severity and frequency of injuries sustained in vehicle rollover is a major public health concern. The National Highway Traffic Safety Administration (NHTSA) addressed these concerns by enacting a federal standard to evaluate rollover crashworthiness using a quasi-static roof crush test (Federal Motor Vehicle Safety Standard 216) despite the fact that rollover is a dynamic event. Public comments to the NHTSA's proposal to upgrade FMVSS 216 criticize the NHTSA's lack of a dynamic test requirement. However, the NHTSA discussed concerns with current dynamic rollover tests stating that they lacked demonstrated repeatability, they did not produce real-world rollovers, and they are not as repeatable as the current quasi-static test in place (NHTSA, 2009). The NHTSA wanted to perform research to address the concerns posted by the public and one of the results was the Dynamic Rollover Test System (DRoTS). Since repeatability was a concern of the NHTSA the goal of this thesis is to evaluate repeatability of the DRoTS relative to standardized crash tests using an objective rating method by presenting two studies followed by a discussion of the limitations of the method and final conclusions.

The first study presents four rollover tests, one pair of late model subcompact sedans and one pair of late model compact multi-purpose vans (MPV), conducted on the DRoTS fixture to evaluate repeatability in terms of initial roof-to-ground contact conditions, vehicle kinematics, road reaction forces, and vehicle deformation. Initial conditions (roll and pitch angle, roll rate, road speed, vertical velocity, mass, and moment of inertia) were found to be 7% different or less while drop height was at most 20mm different in both repeated tests. Plotted data signals of the vehicle response suggest repeatability of the DRoTS fixture however, the measures of repeatability described were subjective and involved qualitative assessments of plotted signals.

The second study used a quantitative approach to assess repeatability of the DRoTS fixture relative to other crash modes. The objective rating method published by the ISO (2014) was used to compare vehicle accelerations, forces, and deformations of frontal, frontal offset, small overlap, small overlap impact (SOI), oblique, deceleration rollover sled (DRS), and DRoTS tests against one another. Based on the average overall rating of the dominant acceleration in each crash mode the crash tests ranked as: 1) Frontal Offset, 2) Frontal, 3) Oblique, 4) SOI, 5) DRoTS, 6) Small Overlap, 7) DRS. As expected frontal crash tests ranked highly when comparing acceleration data and received good repeatability ratings ($R > 0.8$) when comparing reaction force data. DRoTS showed good to excellent ($R > 0.94$) ratings when comparing deformation measures and ranked well above the deformation ratings in SOI tests which all received poor grades. The objective rating method found that the DRoTS tests were as repeatable as other crash modes when comparing the dominant accelerations and showed greater repeatability than the DRS in nearly every other kinematic metric, suggesting that the DRoTS fixture is a highly repeatable dynamic rollover testing device.

Table of Contents

Abstract	iii
List of Figures	vi
List of Tables	vii
Table of nomenclature.....	viii
Introduction	1
Repeatability of the DRoTS Test Fixture.....	4
ABSTRACT	4
INTRODUCTION.....	4
METHODS	5
Vehicle preparation	5
Instrumentation	5
Test Procedure	6
Data Processing.....	7
RESULTS	7
Touchdown Conditions	7
Kinematic Results	8
Boundary Condition Results.....	10
Deformation Results	11
DISCUSSION	13
Tests 1519 vs. 1546.....	13
Tests 1662 vs. 1684.....	14
DRoTS Performance Comparison	16
CONCLUSION	17
Repeatability Study of Replicate Crash Tests: A Signal Analysis Approach	18
ABSTRACT	18
INTRODUCTION.....	18
PREVIOUS STUDIES	19
METHODS	23
RESULTS	25

Small Overlap Impact (SOI) and Oblique Crashes.....	26
Small Overlap	26
Frontal Offset.....	26
Frontal	27
Rollover	28
Examples of Ratings for Deformation, Reaction Load, and Acceleration Signals	29
DISCUSSION	30
Frontal Offset, Small Overlap, SOI and Oblique Crashes	31
Rollover	31
Repeatability Comparison of Crash Tests	33
CONCLUSION	35
Limitations of the ISO Method.....	37
Thesis Conclusions	40
APPENDIX A.....	41
APPENDIX B	43
APPENDIX C	45
APPENDIX D.....	46
APPENDIX E	47
APPENDIX F	48
APPENDIX G.....	51
APPENDIX H.....	53
APPENDIX I	55
REFERENCES	56

LIST OF FIGURES

FIGURE 1. FRONT VIEW HIGH SPEED VIDEO IMAGES, TESTS 1519 VS. 1546 (LEFT), 1662 vs.1684 (RIGHT).....8

FIGURE 2. VEHICLE X ANGULAR VELOCITY AND ROAD VELOCITY, TESTS 1519 VS. 1546 (LEFT) AND TESTS 1662 vs 1684 (RIGHT)9

FIGURE 3. VEHICLE X AND Y ANGULAR DISPLACEMENT, TESTS 1519 VS. 1546 (LEFT) AND TESTS 1662 vs 1684 (RIGHT)9

FIGURE 4. GLOBAL Z' ACCELERATION, TESTS 1519 VS. 1546 (LEFT) AND TESTS 1662 vs 1684 (RIGHT)..... 10

FIGURE 5. GLOBAL Z' VELOCITY, TESTS 1519 VS. 1546 (LEFT) AND TESTS 1662 vs 1684 (RIGHT) .10

FIGURE 6. SUMMED TOTAL VERTICAL REACTION FORCES, TESTS 1519 VS. 1546 (LEFT) AND TESTS 1662 vs. 1684 (RIGHT) 11

FIGURE 7. A-PILLAR RESULTANT AND VEHICLE X, Y, Z COMPONENT DISPLACEMENT TIME HISTORIES (LEFT) AND B-PILLAR RESULTANT AND VEHICLE X, Y, Z COMPONENT DISPLACEMENT TIME HISTORIES (RIGHT) FOR TESTS 1519 VS. 1546..... 12

FIGURE 8. FRONTAL VIEW, TEST 1519 (LEFT) AND 1546 (RIGHT) 13

FIGURE 9. SHORTEST DISTANCE DEFORMATIONS DETERMINED FROM COMPARING PRE- AND POST-TEST LASER SCANNER DATA PLOTTED ON DEFORMED VEHICLE SURFACES FOR TEST 1662(LEFT) AND 1684 (RIGHT). INWARD DEFORMATIONS ARE SHOWN AS NEGATIVE VALUES..... 13

FIGURE 10. TEST 1519 BUMPER MOUNT SHIFT. DASHED OUTLINED ARROWS SHOW ROLL DIRECTION WHILE DOUBLE LINED ARROWS SHOW BUMPER MOVEMENT 14

FIGURE 11: EXAMPLES OF VEHICLE RESULTANT DEFORMATION MEASURES AND THEIR RESPECTIVE CORRELATION VALUES. FROM LEFT TO RIGHT: CHEVY CRUZE SOI TESTS (POOR GRADE), DRoTS SEDAN TESTS (GOOD GRADE), AND DRoTS SEDAN TESTS (EXCELLENT GRADE).....29

FIGURE 12: EXAMPLES OF TOTAL REACTION LOAD MEASURES AND THEIR RESPECTIVE CORRELATION VALUES. FROM LEFT TO RIGHT: DRoTS SEDAN TESTS (GOOD GRADE), FRONTAL TOYOTA COROLLA TESTS (GOOD GRADE), AND FRONTAL HYUNDAI GENESIS TESTS (GOOD GRADE).....29

FIGURE 13: EXAMPLES OF VEHICLE DOMINANT ACCELERATION SIGNALS AND THEIR RESPECTIVE CORRELATION VALUES. FROM LEFT TO RIGHT: SMALL OVERLAP VOLVO S60 (POOR GRADE), FRONTAL OFFSET HYUNDAI ELANTRA TESTS (FAIR GRADE), AND FRONTAL LEXUS RX350 TESTS (GOOD GRADE)30

FIGURE 14: OVERALL RATINGS FOR KINEMATIC AND FORCE SIGNALS FROM ROLLOVER CRASH TESTS33

FIGURE 15: DOMINANT ACCELERATION RATINGS FOR ALL CRASH TESTS, AVERAGE SCORES SHOWN ABOVE RESPECTIVE CRASH TEST34

FIGURE 16: OVERALL RATINGS FOR VARIED SIGNAL TYPES ENCOUNTERED (HIGHLIGHTED BARS INDICATE DRoTS TESTS)35

LIST OF TABLES

TABLE 1. MEASURED TOUCHDOWN PARAMETERS AND MASS PROPERTIES.....	8
TABLE 2. A- AND B-PILLAR PEAK DISPLACEMENTS, TIME OF OCCURRENCE, UNLOADED DISPLACEMENT AND REBOUND	12
TABLE 3: INITIAL CONDITIONS FOR FRONTAL, FRONTAL OFFSET, SMALL OVERLAP, OBLIQUE, AND SOI TESTS	21
TABLE 4: INITIAL CONDITIONS FOR DROTS AND DRS TESTS	23
TABLE 5: OVERALL TEST SIGNAL RATINGS (R) AND GRADES FOR SOI AND OBLIQUE CRASH TESTS	26
TABLE 6: OVERALL TEST SIGNAL RATINGS (R) AND GRADES FOR SMALL OVERLAP TESTS	26
TABLE 7: OVERALL TEST SIGNAL RATINGS (R) AND GRADES FOR FRONTAL OFFSET CRASH TESTS. .	27
TABLE 8: OVERALL TEST SIGNAL RATINGS (R) AND GRADES FOR FRONTAL CRASH TESTS.....	27
TABLE 9: OVERALL TEST SIGNAL RATINGS (R) AND GRADES FOR DROTS AND DRS ROLLOVER CRASH	28

TABLE OF NOMENCLATURE

General

$C, C(t)$	Analyzed Signal
$T, T(t)$	Reference Signal
Δt	Interval between two time samples
t	Time signal
t_0	Time zero
t_{start}	Starting time of the interval of evaluation
t_{end}	Ending time of interval of evaluation
N	Total number of sample points between t_{start} and t_{end}

Corridor

Score

E_z	Corridor score
$Z(t)$	Corridor score at time t
δ_i	Half width of the inner corridor
δ_o	Half width of the outer corridor

EEARTH

General

$C^{\text{ts}}, C^{\text{ts}}(i)$	Truncated and shifted analyzed curve
$C^{\text{ts}+d}$	Derivative of analyzed curve C^{ts}
$C^{\text{ts}+w}$	Warped analyzed curve C^{ts}
$T^{\text{ts}}, T^{\text{ts}}(j)$	Truncated and shifted reference curve
$T^{\text{ts}+d}$	Derivative of reference curve T^{ts}
$T^{\text{ts}+w}$	Warped reference curve T^{ts}
$d(i, j)$	Local cost function to perform the dynamic time warping
m	Time steps moved to evaluate the phase error
ε_p or n_e	Phase offset (number of time shifts to get ρ_E)
ρ_E	Maximum cross correlation of all $\rho_L(m)$ and $\rho_R(m)$
$\rho_L(m)$	Cross correlation – analyzed signal is moved to the left
$\rho_R(m)$	Cross correlation – analyzed signal is moved to the right

Phase score

E_p	Phase score
ε_p^*	Maximum allowable percentage time shift

Magnitude

score

E_m	Magnitude score
ε_m^*	Maximum allowable magnitude error
ε_{mag}	Magnitude error

Slope score

E_s	Slope (topology) score
ϵ_s^*	Maximum allowable slope error
ϵ_{slope}	Slope error

Total ISO rating

R	Total ISO rating
$w_z = 0.4$	Weighting factor of the corridor score E_z
$w_p = 0.2$	Weighting factor of the phase score E_p
$w_m = 0.2$	Weighting factor of the magnitude score E_m
$w_s = 0.2$	Weighting factor of the slope score E_s

INTRODUCTION

According to the National Highway Traffic Safety Administration (NHTSA) Traffic Safety Facts of 2011, rollover crashes contribute more than one-third of all vehicle occupant fatalities, yet rollover occurs in only 2% of all vehicle crashes. The combination of severity and frequency of injuries sustained in vehicle rollover is a major public health concern. Dynamic rollover tests have long been studied to understand vehicle behavior that results from a rollover crash and to evaluate vehicle crashworthiness and occupant protection; however because rollover crashes are complex, and because so many types of crashes can be classified as rollovers, oversimplifying conditions for test procedures results in tests that may not adequately represent real rollover crashes. Additionally, due to the nature of rollover crashes and crash tests, vehicle kinematic response is highly sensitive to variations in initial conditions and vehicle inertial properties (Kerrigan et al. 2011). The federal standard in place for evaluating rollover crashworthiness is a quasi-static roof crush test (Federal Motor Vehicle Safety Standard (FMVSS) 216) despite the fact that rollover is a dynamic event. In an attempt to improve roof crush resistance requirements, the NHTSA conducted 25 full scale dynamic rollover tests using a similar cart design described in FMVSS 208 and used pneumatic cylinders to initiate the vehicle's angular momentum to produce severe roof intrusion. The NHTSA concluded that a dynamic roof crush standard was not feasible due to the severity of roof crush and lack of demonstrated repeatability in occupant kinematics and roof crush (Office of the Federal Register, 2005). Additionally, the NHTSA has commented on the lack of repeatability of the Controlled Rollover Impact System (CRIS) and the Jordan Rollover System (JRS) and questioned their test methods in response to commenters of the FMVSS 216 for use of a dynamic rollover test for rollover crashworthiness (NHTSA, 2009).

According to Copper et al. (2001), the CRIS was developed to controllably “duplicate a wide range of vehicle-to-ground impact configurations,” but vehicle kinematics were not repeatable after initial roof-to-ground impact and no results showing time history comparisons were published. The JRS was created to produce repeatable rollovers (Friedman et al. 2003) and a number of published papers report on the repeatability of the JRS (Jordan et al. 2005, Friedman et al. 2007, Bish et al. 2008). Bish et al. (2008) stated the JRS was highly repeatable based on initial test conditions (Coefficient of variation (COV) less than 16%), variations in peak vertical loads (COV less than 10%), and dummy compressive neck load and N_{ij} (COV equal to 10%). However, the vehicles responded to different initial conditions; drop heights ranged from 86mm to 116mm (30% difference) and roll rates ranged from 182°/s to 223°/s (20% difference). And no vehicle kinematics or occupant response data were reported. Additional dynamic testing was conducted on the Deceleration Rollover Sled (DRS), initially developed to be a non-destructive method to analyze vehicles likeliness to rollover by abruptly decelerating a laterally-oriented vehicle to induce rollover (Rossey et al. 2001). This system was used to conduct a repeatability study of full scale dynamic rollovers which concluded that the DRS was able to produce

repeatable vehicle kinematics when inertially-matched vehicles are subjected to similar test velocities (Kerrigan et al. 2011). While the authors concluded repeatable results based on test conditions, vehicle and occupant response, and vehicle damage, they described the threshold defining repeatability subjectively. In other words, there was no quantitative distinction of what would be considered repeatable and what would be considered not repeatable. The problem with most of the repeatability studies has been in the assessment of repeatability: that repeatability is based on subjective conclusions of data signals, that repeatability is based on static measurements of dynamic tests, or that test inputs were controlled but vehicle response or occupant response did not show repeatability in terms of deformation, variations in peak values, or dummy injury measures. The NHTSA has been criticized for not using a dynamic test to evaluate vehicle crashworthiness which led to the development of the Dynamic Rollover Test System (DRoTS) and therefore a repeatability evaluation is necessary.

Repeatability is inherently subjective since repeated responses will never truly be identical and an acceptable variation between experimental data based on user judgment is needed to suggest successfully repeated tests. As a result, an objective approach to repeatability is needed. Objective rating methods have often been used to quantitatively validate computer aided engineering (CAE) model outputs to physical tests, but have also been used in repeatability and biofidelity studies of crash dummies (Xu et al. 2000) (Nusholtz et al. 2007) (Untaroiu et al. 2013). A number of different objective rating methods exist due to their value in CAE validation and repeatability analysis (Xu et al. 2000, Jacobs et al. 2000, Hovenga et al. 2005; Gehre et al. 2009, ISO 2013). ISO (2013) recently examined four validation metrics based on their potential application to vehicle passive safety, proposed a standard metric using parts of those examined, and demonstrated its effectiveness through cases studies. Since these metrics have been applied to CAE and dummy biofidelity, another extension could be repeatability of vehicle crash tests as objective rating methods evaluate how well two time histories are correlated.

The DRoTS was examined through four full-scale dynamic rollover tests of two pairs of replicate vehicles. The goals of this thesis were to:

1. assess the repeatability of the DRoTS fixture in terms of prescribing test parameters and in terms of the vehicle response to the test parameters
2. use the objective rating metrics proposed by ISO/TR 16250:2013 to compare repeatability of the DRoTS fixture to standardized crash tests through vehicle kinematics, reaction forces, and vehicle deformations

Based upon examination and analysis of prior full scale vehicles tests performed on the DRoTS fixture and regarded as an improvement to the JRS, it is hypothesized that:

1. the DRoTS will show repeatable touch down conditions and repeatable vehicle kinematic, kinetic and deformation responses for replicate vehicle tests.

2. the DRoTS fixture will be as repeatable as other crash modes according to the international standard detailed in ISO/TS 18571:2014, objective rating metrics for non-ambiguous signals.

The following two studies were conducted to meet the goals of this thesis and evaluate the hypotheses. The first study was completed to present a conventional approach to repeatability by conducting tests with replicate subjects. However, since the rollover crash test is more complex than standardized crash tests, a portion of this thesis was committed to characterizing the rollover crash using inertial measurement units to describe the vehicles acceleration in a local and global coordinate system, using string potentiometers to trilaterate deformation time history, and using load cells to measure impact force during the rollover event. These data were used to assess the repeatability of the vehicle response through comparison of peak measurements and time of occurrence of peak values. In the second study, an objective rating method was used to directly compare the repeatability of the DRoTS relative to standardized crash tests. The limitations of the objective rating method are then discussed followed by the overall conclusions of this thesis.

Repeatability of the DRoTS Test Fixture

ABSTRACT

The goal of this study was to evaluate the repeatability of the Dynamic Rollover Test System (DRoTS) in terms of initial roof-to-ground contact conditions, vehicle kinematics, road reaction forces and vehicle deformation. Four rollover crash tests were performed on two pairs of replicate vehicles, instrumented with a custom inertial measurement unit to measure vehicle and global kinematics and string potentiometers to measure pillar deformations. The road was instrumented with load cells to measure reaction loads and an optical encoder to measure road velocity. Laser scans of pre- and post-test vehicles were taken to provide detailed deformation maps. Initial conditions were found to be repeatable, with the largest difference seen in drop height of 20mm while roll rate, roll angle, pitch angle, road velocity, drop velocity, mass, and moment of inertia were all 7% different or less despite initial issues with the trigger release. Improvements of the test equipment and matching mass properties will ensure highly repeatable initial conditions, vehicle kinematics, kinetics, and deformations.

INTRODUCTION

Vehicle rollover crashes are a major occupant safety concern and have long been studied in a variety of ways, from corkscrew ramp methods to side curb tripping methods to dolly rollover tests, in order to understand vehicle response, occupant/vehicle interaction and mitigation techniques. However, there is no dynamic test standard partially because the National Highway Traffic Safety Administration (NHTSA) has indicated repeatability has not yet been demonstrated (Office of the Federal Register, 1999).

Repeatability issues have led to new systems to assess rollover crashes through dynamic evaluations, such as the Controlled Rollover Impact System (CRIS) (Cooper et al. 2001), the Jordan Rollover System (JRS) (Friedman et al. 2003), and the Deceleration Rollover Sled (DRS) (Rossey et al. 2001). However, test methods of fixtures claimed to be repeatable such as the CRIS and JRS, were based on little evidence (Moffatt et al. 2003, Bish et al. 2008). Kerrigan et al. (2011) looked at 5 different metrics (touchdown conditions, input kinematics, vehicle kinematic response, vehicle deformation, and dummy response) and some objective rating techniques to suggest that repeatability of the DRS was observed when vehicle inertial properties were very similar.

The DRoTS was developed as a research tool to examine some of the conditions that occur in real rollover crashes in a controlled, repeatable laboratory environment. This study performed a similar analysis to the DRS study as described by Kerrigan et al. (2011) in which repeatability of initial conditions, vehicle kinematics, road reaction forces and vehicle deformations were analyzed

METHODS

Four rollover impact tests were performed with two pairs of replicate vehicles (tests 1519 and 1546: subcompact sedan, tests 1662 and 1684: compact multi-purpose van (MPV)) using UVA's Dynamic Rollover Test System (DRoTS). All vehicles were prepared for testing using a standard procedure that included loading each vehicle into the DRoTS fixture (Kerrigan et al. 2013). Once loaded, timing tests were performed to finalize test parameters and then the rollover impact tests were conducted. After testing, damage to the vehicles was assessed and test data were processed and analyzed.

Vehicle preparation

After receiving each vehicle the mass distribution and total mass were recorded. Since mounting hardware, instrumentation, and data acquisition were to be added to each vehicle, vehicle components were removed and fluids were drained in an effort to achieve a target mass and mass distribution for each vehicle:

- Tests 1519 (sedan1) and 1546 (sedan2) - No specific target mass was required except to match the mass and mass distribution between tests. As much mass was removed as possible to accommodate the 139.3kg cradle and 41.2kg mounting hardware (Kerrigan et al. 2013) without compromising the vehicle structure.
- Test 1662 (MPV1) - Since the second MPV test was to have driver and right front passenger dummies, a target mass for the first MPV was determined by adding all of the instrumentation and data acquisition components related to dummies to MPV1. Before removing the front seats the mass distribution was measured with two human volunteers (approximately 50th percentile male) seated in the driver and right front passenger seats. This mass distribution was then achieved after removing internal components and adding ballast to accommodate difference in mass.
- Test 1684 (MPV2) – Target mass and mass distribution were matched closely to MPV1 with dummies positioned in the driver and right passenger front seats.

In order to interface test vehicles to the DRoTS fixture, vehicles were prepared using techniques similar to those previously described (Kerrigan et al. 2011 SAE, 2013). Custom hardware was fabricated to rigidly attach the DRoTS cradle to the front and rear bumper beam mounts after removing the fascia and bumper beams (exception for tests 1519 and 1546 where bumper beams were modified).

Instrumentation

Data acquisition systems and related components, instrumentation, cameras, lights and imaging system components were added to each vehicle to facilitate data acquisition and photography. Each vehicle was instrumented with a custom inertial measurement unit (IMU) consisting of accelerometers and angular rate sensors and was mounted rigidly to the floor on the lateral center line with an approximate alignment of the IMU's local x-axis to the vehicle's roll axis. Test 1519 and 1546 used an IMU containing three different types of accelerometers: a 2000 g piezoresistive

sensor (Endevco 7264B-2000, Meggitt Sensing Systems, San Juan Capistrano, CA), a gas-damped 20 g silicon MEMS sensor (MSI 4000A, Measurement Specialties Inc., Hampton, VA), and a gas-damped 30 g variable capacitance sensor (Endevco 7290E-30, Meggitt Sensing Systems, San Juan Capistrano, CA). Three accelerometers of each of the three types were mounted on three mutually perpendicular planes of the IMU, to measure the IMU's local x, y, and z component accelerations. Three angular rate sensors were also mounted perpendicularly: a 1500 °/s sensor on the IMU's local x-axis and two 300 °/s sensors on the other axes (DTS ARS, Diversified Technical Systems, Seal Beach, CA). For Tests 1662 and 1684, a new custom IMU was machined but held all of the original sensors of the first IMU in addition to six accelerometers (2000 g piezoresistive sensors (Endevco 7264B-2000, Meggitt Sensing Systems, San Juan Capistrano, CA)), which were installed to facilitate calculation of the vehicle angular acceleration by standard nine-accelerometer-package processing techniques (DiMasi, 1995).

Other vehicle sensors included six string potentiometers (model 62-60, Firstmark Controls, Creedmoor, NC) attached to the vehicle floor and two triaxial accelerometers (Endevco 7267A, Meggitt Sensing Systems, San Juan Capistrano, CA) attached to a mounting plate at the driver's side A- and B-pillars. Each set of three potentiometers extended from the vehicle floor to mounting plates installed on the roof rail near the driver's side A- and B-pillars. No deformation measurement sensors were installed in MPV2, so while sensors were installed in MPV1, these data were not presented since no comparison can be made.

The DRoTS test fixture also utilized a number of sensors to monitor system performance and to collect test data. In particular, twenty uniaxial load cells (SWP-20K, Transducer Techniques, Temecula, CA) were mounted in the roadbed to measure forces normal to the roadbed surface. Four string potentiometers were also attached to the DRoTS test fixture and extended to the control arms for the MPV tests to measure the drop height, drop velocity and pitch rate. An optical encoder (model 725, Encoder Products, Sagle, ID) was attached to the road propulsion system and used to measure the road velocity.

Test Procedure

The test procedure used in these tests has been previously described (Kerrigan et al. 2013). Briefly, once vehicle preparation was completed and the vehicle was fully instrumented, it was attached to the DRoTS control arms, final adjustments to the control tower were made, and ballast was added if needed to ensure rotational stability. The moment of inertia (MOI) was calculated by conducting a roll-only (non-contact) test while collecting the force needed to rotate the vehicles and the angular roll rate of the vehicle. Once the MOI was calculated, speed tests were run to adjust timing of roll initiation and drop release after the roadbed passed the event trigger to ensure accurate touchdown conditions. Touchdown conditions of the second sedan test were chosen to match the first sedan test (previously described (Kerrigan et al. 2013)). MPV test conditions were based on a reconstruction of a National Automotive Sampling System Crashworthiness Data System (NASS-CDS) case number 2008-03-108 performed with computational modeling.

Before the final test a coordinate measurement machine (CMM) (Titanium Arm, FARO Technologies, Lake Mary, FL) was used to facilitate kinematics data processing. Additionally,

the vehicle exterior of each test was scanned with a commercial laser scanner (Focus 3D, FARO Technologies, Lake Mary, FL) to obtain a point cloud description of the vehicle exterior pre- and post-test for deformation measures.

Data Processing

Kinematics Data Processing

All sensor data were filtered and debiased and were time shifted such that time $t=0$ corresponded to the time of touchdown. Road and control arm load cells, vehicle accelerometers, and string potentiometers, were filtered to CFC60 and vehicle angular rate sensors were filtered to CFC180 (SAE, 1995). The filtered and debiased IMU signals were used to compute vehicle and global center-of-gravity (CG) linear and angular accelerations, velocities, and displacements using rigid body kinematics in conjunction with a method of computing vehicle-to-global coordinate transformation time histories formulated by Beard and Schlick et al. (2003). Complete kinematic data analysis processing has been previously outlined in detail (Kerrigan et al. 2013). Vehicle coordinate system follows SAE J1733 standard vehicle coordinate system (+X-axis from rear bumper to front bumper, +Y-axis from driver side to passenger side, +Z-axis from roof to floor). Global coordinate system was: +X'-axis is direction of road travel, +Z'-axis is directed towards the ground, and +Y-axis is cross product of +Z-axis with +X'-axis.

Deformation Data Processing

A trilateration algorithm was applied to string potentiometer data from the sedan tests to determine the component-wise (vehicle X, Y, and Z) displacements of the point tracked on the interior of the car's surface. The methodology for this calculation and a validation of the technique has been previously described (Kerrigan et al. 2013).

Deformation contours were created using 3D inspection and metrology software (Geomagic Qualify 12, Geomagic Technologies, Research Triangle Park, NC), 3D point cloud software (Faro Scene 5.0, FARO Technologies, Lake Mary, FL) and point cloud data captured with a commercial laser scanner (Focus 3D, FARO Technologies, Lake Mary, FL).

RESULTS

Touchdown Conditions

For tests 1519 and 1546 most touchdown conditions closely matched test parameters with respect to one other. Largest percent difference was calculated at 7% for pitch angle at touchdown while all other parameters were within 5% difference (Table 1). Touchdown conditions for tests 1662 and 1684 were also very similar. The largest variations in test parameters were the drop height (14% or 20mm) and vertical velocity (7%, or 0.12m/s) due to a 2% difference in roll angle (Table 1).

Table 1. Measured touchdown parameters and mass properties

Test Numbers	1519	1546	% Diff.	1662	1684	% Diff.
Pitch Angle (°)*	-12.8	-11.9	7%	-7.7	-7.5	3%
Roll Angle (°)*	181.0	181.0	0%	-143.2	-146.2	2%
Roll Rate (°/s)*	268	274	2%	-245	-248	1%
Road Speed (m/s)	8.38	8.52	2%	7.54	7.54	0%
Vertical Velocity (m/s)	1.91	1.84	4%	1.67	1.55	7%
Drop Height (mm)	247	234	5%	158	138	14%
Mass As Tested (kg)	1173.9	1181.6	1%	2260.2	2257.6	0%
MOI (kg m ²)	379	378	0%	980	1002	2%

*Pitch and roll angles are expressed in the SAE vehicle coordinate system with negative front-down pitch and positive roll angles in the passenger-side leading direction.

Kinematic Results

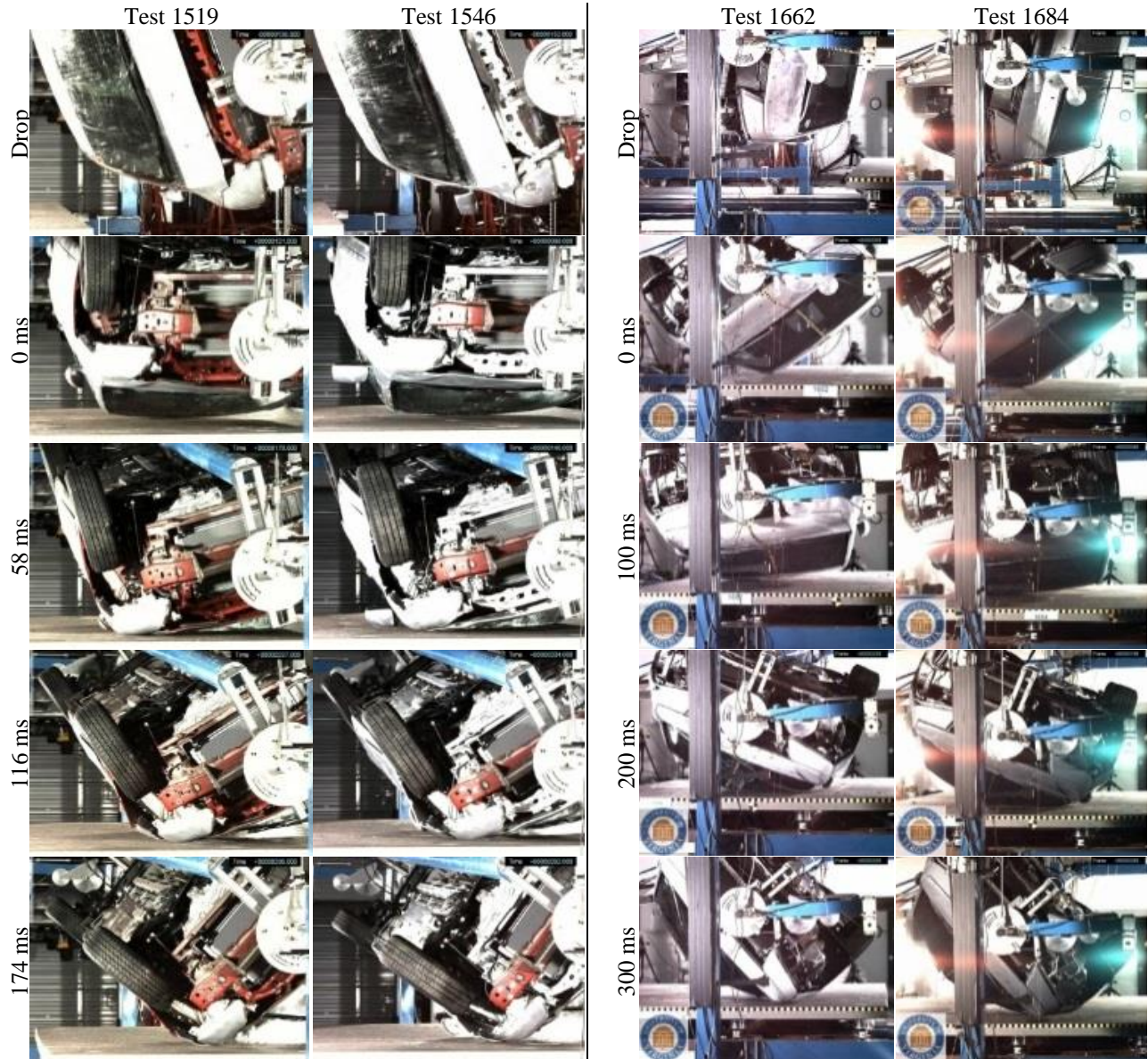


Figure 1. Front view high speed video images, tests 1519 vs. 1546 (left), 1662 vs.1684 (right).

Selected vehicle kinematic data for tests 1519, 1546, 1662, and 1684 are presented (Figure 2- Figure 5), which corresponds to the vehicle motions (Figure 1); complete kinematic data are shown in Appendices A and B. Despite having very similar roll rates initially, the vehicle in test 1546 showed an increase in roll rate beginning at 70ms relative to test 1519, with roll rates exceeding $50^{\circ}/s$ (17%) more than test 1519 throughout the impact. Road velocities remained similar until 116ms, where test 1519 slows down slightly and remains consistently slower than in test 1546. Vehicle X and Y angular displacements show strong correlations between tests (Figure 3), although vehicle Y angular displacement was consistently (around 1.5° for impact duration) higher in test 1519.

Similar roll rates were seen initially in 1662 and 1684 however, the vehicle in test 1662 had a greater roll rate during the first 130ms after touchdown with the peak difference between tests exceeding $39^{\circ}/s$ (6%) around 128ms. Road velocities remained similar until 116ms, where 1684 slows down faster than in test 1546. Vehicle X angular displacements remained nearly identical while vehicle Y angular displacements varied more over time.

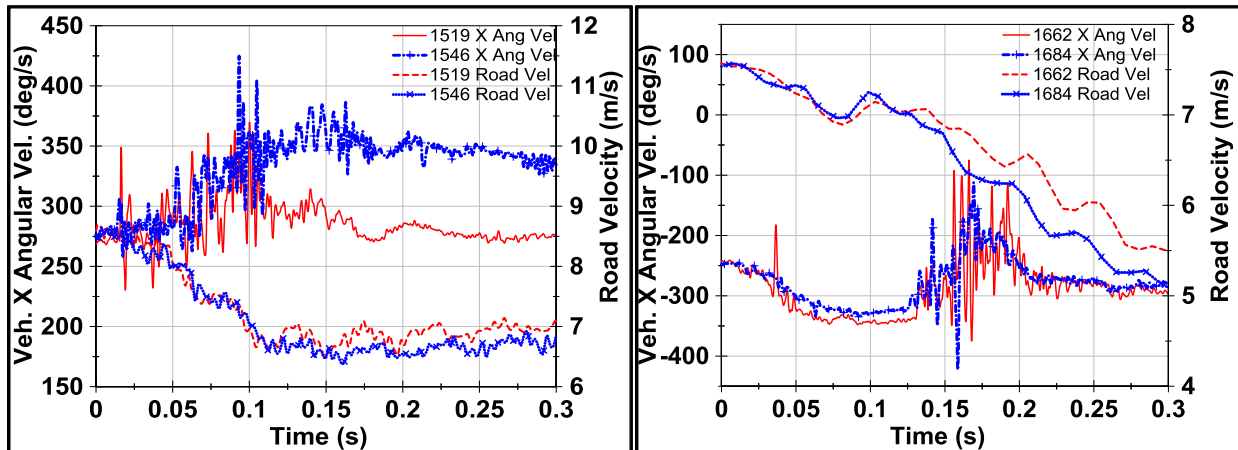


Figure 2. Vehicle X angular velocity and road velocity, tests 1519 vs. 1546 (left) and tests 1662 vs 1684 (right)

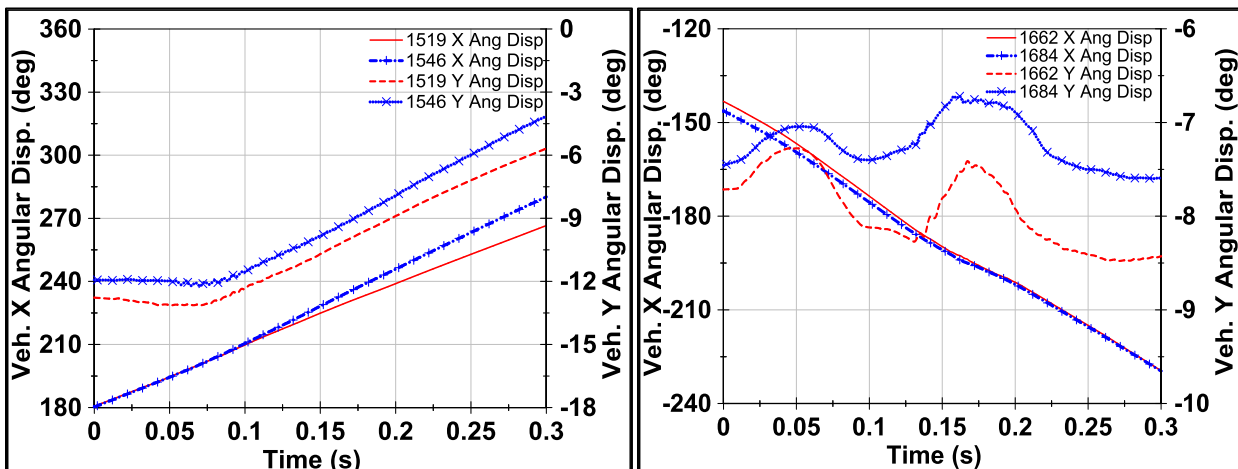


Figure 3. Vehicle X and Y angular displacement, tests 1519 vs. 1546 (left) and tests 1662 vs 1684 (right)

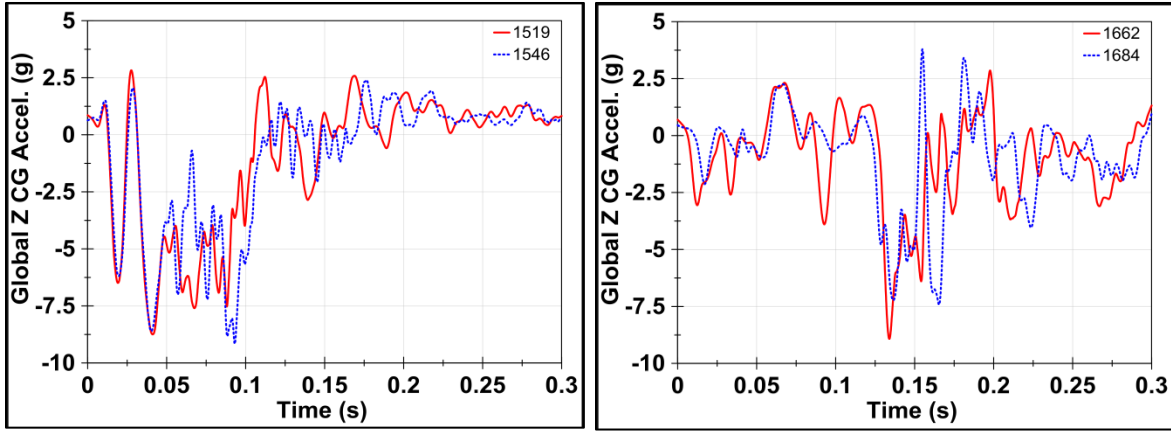


Figure 4. Global Z' acceleration, tests 1519 vs. 1546 (left) and tests 1662 vs 1684 (right)

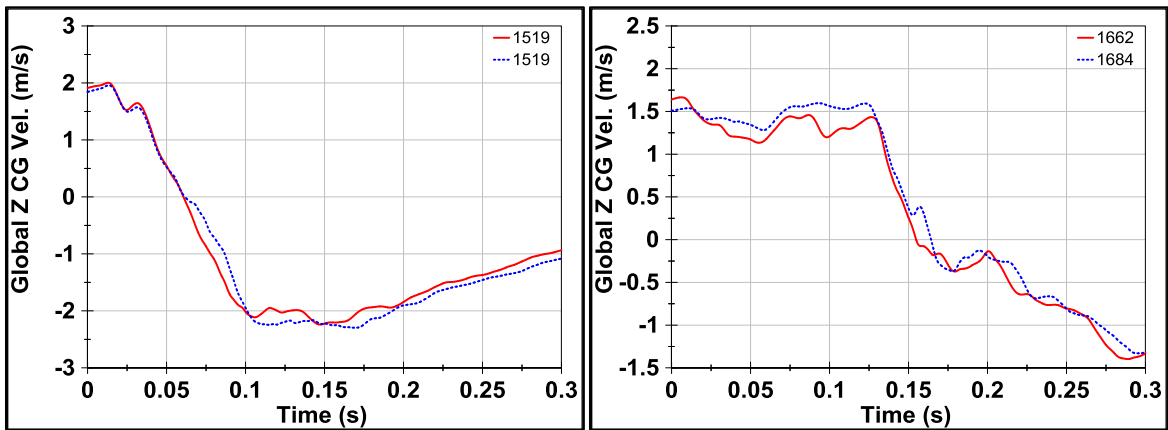


Figure 5. Global Z' velocity, tests 1519 vs. 1546 (left) and tests 1662 vs 1684 (right)

Boundary Condition Results

Road reaction forces were similar for both paired tests, but data acquisition problems affected the response data for tests 1662 and 1684. In 1662, the road's data acquisition system ceased functioning at approximately 0.155 seconds. As a result, load time history data are truncated there (Figure 6). In 1684, the data acquisition system temporarily failed at about 163ms, which was evidenced by all the load cells temporarily reading negative rail. Despite these problems, peak loads differed by less than 7000 N (4%) and 2ms. The peak force in 1662 was slightly higher than in 1684 (177.4kN vs. 170.7kN). The peak force occurred within 2° of the same roll angle (189.6 vs. 187.9). For tests 1519 and 1546, peak loads differed by 11.7% (94.4kN vs. 84.0kN) and 4ms, which occurred within 1.3° of the same roll angle (196.2 vs. 194.9).

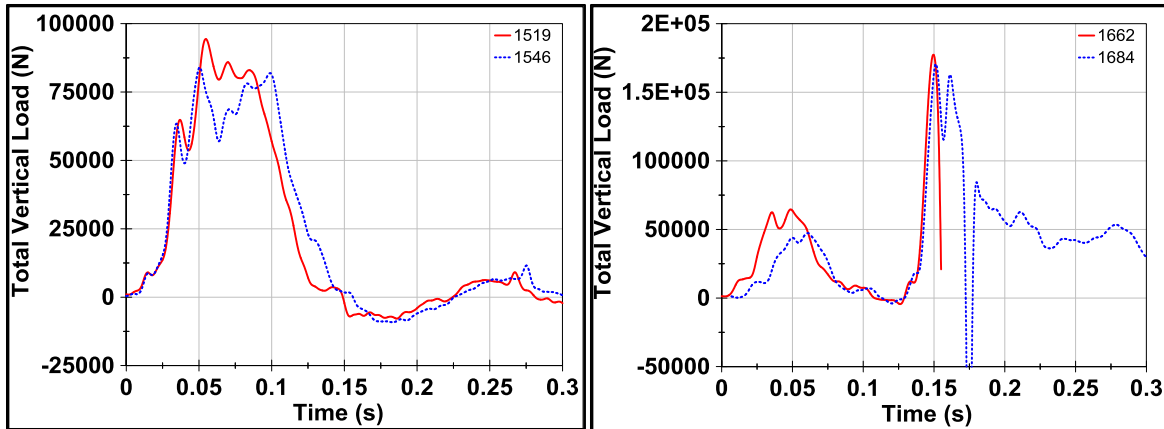


Figure 6. Summed Total Vertical Reaction Forces, Tests 1519 vs. 1546 (left) and Tests 1662 vs. 1684 (right)

Deformation Results

The peak resultant deformation at the top of the A-pillar for test 1519 was 222 mm at 86ms and for test 1546 was 219 mm at 86.1ms: a 0.4% difference in magnitude and only 0.1ms difference in timing (Figure 7). Throughout the loading of the A-pillar, deformations remained mostly in the vehicle's Y-Z plane, with peak Z deformations (168 - 163mm) slightly higher than peak Y deformations (146-148mm). Differences in peak between the tests were largest (31%) in the X direction since small deformations occurred in opposite directions, with Y and Z peak deformation differences remaining relatively low (1-3%). Although the percent difference was large, the difference in displacement between peaks was only 7mm. Unloading of the A-pillar showed nearly twice as much rebound in vehicle Y-direction (45 – 51%) than in the vehicle Z-direction (26-29%) despite initial contact of 181° (Table 2).

The maximum resultant deformation at the B-pillar for test 1519 was 132 mm at 84ms and for test 1546 was 149.9mm at 86.8ms: a 13% difference in magnitude and 2.8ms difference in timing (Figure 7). Throughout the loading of the A-pillar, deformations remained mostly in the vehicle's Y-Z plane, with Z deformations slightly higher than Y deformations up until around 62ms. After 62ms, Y deformations exceed Z deformations, reaching peak values of 105 – 123 mm at around 86ms while Z deformations peaked to 86 mm at 59ms and 92mm at 77ms. Differences in peak between the tests were largest (57% or only 15mm) in the X direction since small deformations occurred in opposite directions, with Y and Z peak deformation differences remaining relatively low (16% and 7%). Rebound of the B-pillar was not as pronounced as in the A-pillar due to level of deformation however, similarly to the A-pillar, rebound of the vehicle Y deformations (48-51%) were greater than rebound of the vehicle Z deformations (39-45%) (Table 2).

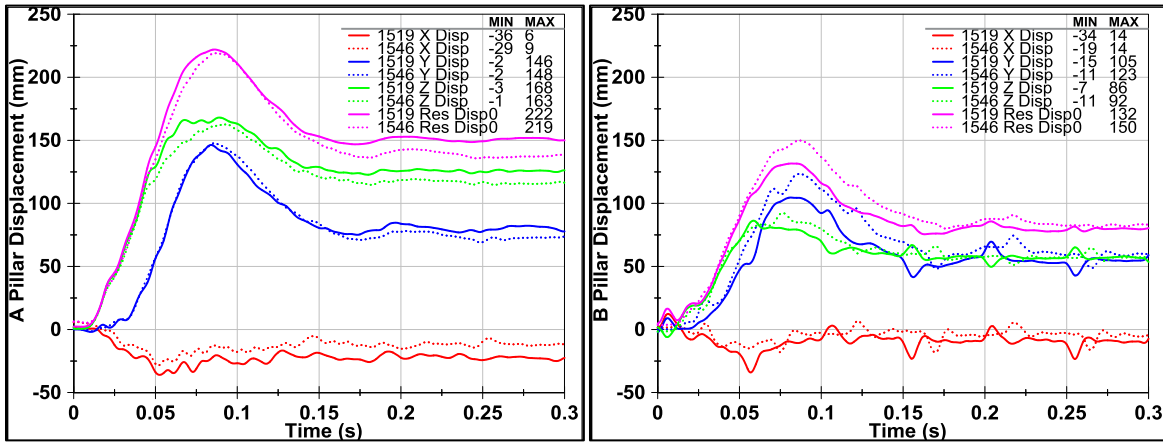


Figure 7. A-pillar resultant and vehicle X, Y, Z component displacement time histories (left) and B-pillar resultant and vehicle X, Y, Z component displacement time histories (right) for Tests 1519 vs. 1546

Table 2. A- and B-pillar peak displacements, time of occurrence, unloaded displacement and rebound

	Peak Disp. (mm)			Time at Peak (ms)		Unloaded Disp. (mm)			Rebound	
	1519	1546	% Diff	1519	1546	1519	1546	% Diff	1519	1546
Ax	-36	-29	31%	52.6	51.6	-21	-12	55%	42%	59%
Ay	146	148	1%	84.1	85.9	80	73	9%	45%	51%
Az	168	163	3%	88.9	93.2	125	116	7%	26%	29%
Ar	222	219	1%	86	86.1	151	138	9%	32%	37%
Bx	-34	-19	57%	56.8	74.8	-9	-5	57%	74%	74%
By	105	123	16%	85.8	86.7	55	60	9%	48%	51%
Bz	86	92	7%	58.6	76.5	57	57	0%	34%	38%
Br	132	150	13%	84	86.8	80	83	4%	39%	45%

Laser scans were conducted on tests 1519 and 1546 however deformation plots were not generated due to a lack of common targets for accurate alignment of pre- and post-test scans. Instead, vehicle frontal images are shown depicting similar deformations in the roof (Figure 8). Contour plots depicting the shortest distance between the original (pre-test) and deformed (post-test) surfaces are plotted on the deformed surfaces for 1662 and 1684 (Figure 9). The shortest distance deformation maps show highly similar deformations between the two vehicles with portions of the passenger side A-pillar and A/B roof rail sustaining permanent deformations approaching 120mm. Significant outward deformations were seen near the centerline of the vehicle roof (approaching 80mm), but the leading side roof rail only sustained minimal outward deformations.



Figure 8. Frontal view, Test 1519 (left) and 1546 (right)

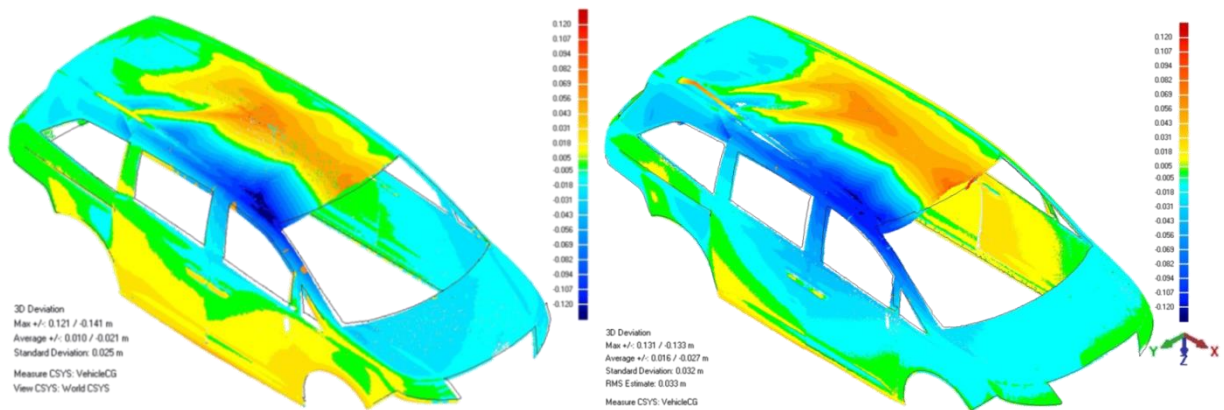


Figure 9. Shortest distance deformations determined from comparing pre- and post-test laser scanner data plotted on deformed vehicle surfaces for test 1662(left) and 1684 (right). Inward deformations are shown as negative values.

DISCUSSION

Tests 1519 vs. 1546

In test 1519, the mechanism that releases the vehicle from a fixed, to a free-fall state, just before the initial roof to ground contact, had a failure (Kerrigan et al. 2013). As a result of this problem, the drop release system was redesigned before performing the next test; however differences between actual touchdown conditions of the sedan tests were 7% or less.

During test 1519, video images of the front bumper (Figure 10), which was used to fix the vehicle to the test fixture cradle, showed abrupt movement in the vehicle local Y-direction relative to the vehicle frame. Video analysis showed sudden movement at 83ms followed by another sudden shift at 95ms. Abrupt changes in the vehicle local X angular velocity data were also be seen at similar times, where at approximately 83ms the vehicle angular rate decreased for a few milliseconds (deviating from increasing rate data in test 1546) and then increased until 95ms when it began to decrease again (Figure 2). Additionally, other kinematic descriptions showed deviation after 83ms; global Z' accelerations were not affected and nearly identical

(Figure 4) while global X' accelerations were strongly correlated up until this time (Appendix A) and vehicle Z angular rate data deviates after 95ms (Appendix A). The bumper beam's motion relative to the vehicle caused the roll axis to move away from the vehicle's center of gravity, which resulted in an imbalance of the vehicle's rotation. The imbalanced rotation resulted in a higher roll moment of inertia, which explains the reduced roll rate after the motion in the first sedan test (1519).

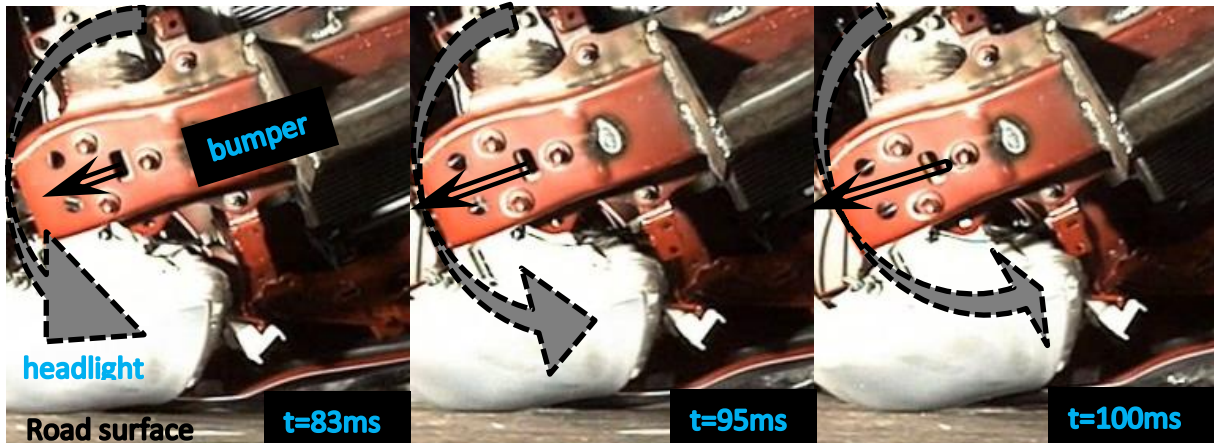


Figure 10. Test 1519 bumper mount shift. Dashed outlined arrows show roll direction while double lined arrows show bumper movement

Overall, the total vertical force and deformation data showed strong correlations between repeated tests however, differences were seen starting at 50ms, when the vertical force in test 1519 surpassed the peak force in test 1546 for 40ms. The increase in force of test 1519 caused more deformation at the B-pillar relative to test 1546 (150mm vs. 132mm), while component deformations of the A-pillar were very similar between tests. This increase in force was likely due to the larger pitch angle (-12.8° vs -11.9°) and drop height (247mm vs. 234mm) during test 1519 which would cause the increased global Z' CG velocity (Figure 5) and vehicle angular Y velocity (Appendix A) after 60ms. The bumper motion, which was hypothesized to have caused the variation in kinematics, did not appear to cause variations in the contact force and vehicle deformation.

Since the resulting kinematics seem to be well correlated before 83ms, and a shift of the vehicle CG from the roll axis accounts for the changes seen after 83ms, and that no variations or divergences were observed in the force or deformation data at that time, it was expected that vehicle response during a DRoTS test can be more repeatable if the roll axis is maintained.

Tests 1662 vs. 1684

To resolve the issue identified in test 1519, after the small sedan test series, all future test vehicles utilized direct connection, through custom hardware, between the vehicle frame rails and the DRoTS cradle, without use of the bumper beam. The MPV tests initiated impacts on the leading side and then had a trailing side impact as noticed by the bimodal shape of the vertical force data (Figure 6), whereas the sedan tests only had trailing side impacts. Unlike the sedan

tests, initial conditions of the MPV tests exceeded 7% difference in drop height alone (14%, 158 vs 138mm) while all other touch down conditions were 7% or less.

Despite only 3°/s difference in roll rate at touchdown and both vehicles increased their roll rates during the interaction between the road and the leading side of the vehicle, the vehicle in 1662 endured a slightly higher increase in roll rate. The maximum difference in roll rate was 39°/s which occurred at 128ms. Despite the 39°/s difference between the two vehicles upon initiation of the trailing side impact, both vehicles roll rates decreased to the same level, and generally tracked each other without significant variation for the remainder of the test. It was hypothesized that the first vehicle achieved a higher roll rate during the initial contact phase was related to a 2.2% difference in moment of inertia (980kg m² in 1662 and 1002kg m² in 1684). Since the vehicle's roll rate increased initially as a result of frictional forces from the faster moving road (road speed was 7.5m/s while tangential speed of the vehicle was only 5.4m/s), a greater increase in roll rate would be expected in the case where the vehicle had a lower moment of inertia. Since the roll angle was slightly (3°) higher at touchdown in the case of 1684, the increased roll rate in 1662 resulted in the 3° difference gradually becoming a 0° difference by 310ms. However, from a simplified energy analysis the increase in rotational energy of the vehicle in 1662 (7771J) during the leading side impact was 13% larger than the increase in rotational energy of the vehicle in test 1684 (6857J), which could not be produced by 2.2% difference in MOI between tests. The impact force exerted on 1662 during the leading side contact was consistently larger than the force exerted on the vehicle in 1684 with a max difference of 17kN until the trailing side contact of 1684 which occurred 119ms later (Figure 6). This was likely due to 1662 landing earlier during its rotation which caused a stiffer load path than for 1684. As the vehicles continued to roll, the force experienced on both diminished at the same rate because the effective distance from the CG to the roof decreased faster than the vehicles were falling, limiting the contact between the roof and the road. During the trailing side impact, both vehicles experienced a similar loading rate and peak force. The offset of the leading side impact force was the likely cause for 1662 to initially achieve a higher roll rate than 1684 which allowed 1662 to impact the trailing side at a similar time to 1684.

Similarly, there was a slight difference in the Y-axis rotational kinematics between the two tests, but this only manifested in a maximum of less than 1° difference in the pitch angle throughout the portion of the test where the vehicle roof was loaded. In general, the shape of the angular acceleration and angular velocity time histories between all three components were very similar (Appendix B), showing that the vehicle and test condition exhibited a highly repeatable result.

Road motion showed very good repeatability between the MPV tests (Figure 2). The rate of deceleration of the road as a result of vehicle loading was very similar between the two tests, however, the road slowed down less in the case of 1662 than in 1684 during trailing side impact. This result was consistent with the hypothesis that the increased roll rate in 1662 was the result of the lower vehicle moment of inertia. Since the moment of inertia was smaller in 1662, less energy was required to increase the roll rate by the same amount as compared to 1684, and thus the road slowed down less in 1662 (since it gave up less of its energy to the roll).

Additionally, differences in CG location may have also caused differences seen in selected data channels. Due to supplemental studies performed in 1684, ATD's were positioned in the driver

and right front passenger seats and different vehicle components were not removed, as they were in 1662. Although efforts were made to reduce differences in mass and mass distribution, the CG location still moved 53.5mm (44mm X-dir., -11.4mm Y-dir., -28.2mm Z-dir.) relative to 1662. The CG moved because the masses used as ballast in place of the occupants in 1662, was added to the floor, and not as high as the occupants, thus the CG in 1684 was higher (as the -28 mm in Z shows). This supports the findings of Kerrigan et al. (2011), in which variation of vehicle CG location may have a significant effect on vehicle response.

Though dynamic deformation data was not collected for both MPV tests, deformation contours of both tests showed very similar deformation patterns and values (Figure 9). Passenger roof rail deformation in 1662 (contour levels between 94mm and 107mm) matched closely to final resultant dynamic deformation at the A- (92mm) and B-pillars (107mm). Between MPV tests, 1662 showed slightly larger deformations in the passenger roof rail which correlates to slightly higher peak reaction forces on the trailing side for 1662 (177kN vs. 171kN).

DRoTS Performance Comparison

MPV tests were not seen to exhibit any mechanical abnormalities during impact, whereby proper fixation of the vehicles solved the problem that occurred with the sedan1 test and the DRoTS showed very repeatable results. As opposed to repeatability studies of the CRIS and JRS fixtures, complete time history data of vehicle kinematic, kinetic, and deformations responses of replicate tests were presented and showed high levels of repeatability. Even compared to the DRS study, dynamic and static deformations as well as vertical reaction force time histories provided more detail about the repeatability of the vehicle response in a DRoTS test.

The variation in touchdown conditions of DRoTS tests was very similar to the touchdown conditions using the CRIS presented by Moffatt et al. (2003); roll angle, roll rate, and translational velocity all had a percent difference of 2% or less and both test systems had larger differences in drop height, 10% max difference (269mm vs. 297mm) with CRIS and 14% max difference (158mm vs. 138mm) with DRoTS fixture. Moffatt et al. concluded that the CRIS was a repeatable dynamic rollover test system based on ATD measures of Fz neck compression (max 10% difference) and neck injury (max 4% difference). Thus, by translation the DRoTS fixture can be expected to show at least similar differences in dummy response if dummies were to be used in DRoTS tests.

In addition, variation in touchdown conditions of DRoTS tests was small compared to rollover tests conducted using the JRS presented by Bish et al. (2008). Though roll angle, pitch angle, and translational velocity all had a percent difference of 2% or less in tests using the JRS, the max percent difference in drop height was 30% and roll rate was 20%. These large differences influenced the variation in dummy injury measures with max percent differences in neck compression of 17% and neck injury of 21%, which was to be expected. This further supports the conclusion that the DRoTS would be expected to show relatively small variation in dummy injury measures between repeated tests.

Currently, evaluation of the repeatability of occupant response cannot be conducted as only 1 of the 4 tests had occupants. Further investigation of the DRoTS fixture will be conducted to

evaluate repeatability of dummy responses, as seen in the DRS study by Kerrigan et al. (2011), since this will be an essential evaluation for studying occupant safety during a rollover event. Similar to the analysis conducted by Kerrigan et al. (2011), an objective rating method should be used to correlate data signals in repeated tests to quantitatively distinguish repeatability of vehicle and occupant responses. However, previous evaluations have subjectively defined repeatability since a repeatability benchmark in rollover does not exist. This was seen in the JRS studies where repeatability of the system was based on visual comparison and peak values of reaction forces and max roof intrusion measures rather than quantitatively comparing data signals between tests. Although the DRS study used an objective rating method, a threshold for repeatability was not established which lead to subjective conclusions. The use of subjective analyses, as what has been presented, was sufficient for comparing vehicle responses between pairs of tests, but to compare between test methods (vs. DRS or vs. JRS) and to establish a repeatability benchmark, an objective rating will be necessary and should be considered for future use.

CONCLUSION

This study presented the results from two pairs of repeated tests conducted on the DRoTS test fixture aimed to determine how well the DRoTS can prescribe identical test conditions to replicate vehicles and to characterize vehicle response to a rollover test on the DRoTS fixture. Repeatability of the test fixture was evaluated by comparing initial parameters at roof to ground contact between replicate tests as well as analyzing sensor data describing vehicle kinematics, kinetics, and deformations.

Both paired tests showed that the DRoTS was able to repeatedly prescribe initial conditions to vehicles during a rollover test. In the sedan tests, a problem with vehicle fixation to the test fixture caused a divergence of vehicle kinematics after the first 83ms of interaction. This did not, however, have an effect on the deformation or forces measured in the test. The vehicle fixation problem was corrected for the van tests, which showed very similar kinematics, kinetics, and deformations. This study shows that the DRoTS can be used to repeatedly evaluate rollover crashworthiness; therefore an objective approach would strengthen these findings and would allow for evaluating repeatability of DRoTS relative to other test modes.

Repeatability Study of Replicate Crash Tests: A Signal Analysis Approach

ABSTRACT

To provide an objective basis on which to evaluate the repeatability of vehicle crash test methods, a recently developed signal analysis method was used to evaluate correlation of sensor time history data between replicate vehicle crash tests. The goal of this study was to evaluate the repeatability of rollover crash tests performed with the Dynamic Rollover Test System (DRoTS) relative to other vehicle crash test methods. Test data from DRoTS tests, Deceleration Rollover Sled (DRS) tests, frontal crash tests, frontal offset crash tests, small overlap crash tests, Small Overlap Impact (SOI) crash tests, and Oblique crash tests were obtained from the literature and publicly available databases (the National Highway Traffic Safety Administration vehicle database and the Insurance Institute for Highway Safety TechData) to examine crash test repeatability. Signal analysis of the DRoTS tests showed that force and deformation time histories had good to excellent repeatability, while vehicle kinematics showed only fair repeatability due to the vehicle mounting method for one pair of tests and slightly dissimilar mass properties (2.2%) in a second pair of tests. Relative to the DRS, the DRoTS tests showed higher levels of repeatability in nearly all vehicle kinematic data signals with the exception of global X' (road direction of travel) velocity and displacement due to the functionality of the DRoTS fixture. Based on the average overall scoring metric of the dominant acceleration, DRoTS was found to be as repeatable as all other crash tests analyzed. Vertical force measures showed good repeatability and were on par with frontal crash barrier forces. Dynamic deformation measures showed good to excellent repeatability as opposed to poor repeatability seen in SOI and Oblique deformation measures. Using the signal analysis method as outlined in this paper, the DRoTS was shown to have the same or better repeatability of crash test methods used in government regulatory and consumer evaluation test protocols.

INTRODUCTION

Concurrently, repeatability of the Dynamic Rollover Test System (DRoTS) was evaluated relative to initial roof-to-ground contact conditions, vehicle kinematics, road reaction forces, and vehicle deformations. The results showed that variations in all initial contact conditions were less than 10% for both sets of repeated tests. Global Z' acceleration and velocity (drop direction) matched closely for both pairs of tests, angular roll velocity and road velocity initially were similar but deviated within the first 100ms in both pairs of tests, and vertical force data were similar in both cases. While the test fixture was found to exhibit a high level of repeatability, the

assessment of repeatability was subjective. Such subjective evaluations have been performed before for rollover test procedures, namely CRIS and JRS, as well as for other crash test modes including frontal, frontal offset, small overlap, small overlap impact (SOI) and offset Oblique.

Repeatability studies have lacked a methodology to quantify the level of repeatability of experimental tests, often leading to conclusions with subjective bases. Attempts to assess repeatability have examined variations in peaks of time history data, through visual inspection of time history or deformation data, or through variations of single value measures (ie. pre- to post-test displacements of components in the occupant compartment). These evaluations of time history data lack description of the characterization of the data signals. Therefore, a signal analysis approach to quantify the topology of time history data is needed to fully assess repeatability of test signals.

Objective ratings metrics for vehicle crashes have been long studied in order to quantify fidelity between computational simulation and test data. Additionally, correlation analysis has been studied to evaluate repeatability of Hybrid-III and THOR dummies (Xu et al. 2000) and has also been used by ISO/TC 22/SC 10 and 12 to assist in biofidelity analysis of side impact dummies (Gehre et al. 2009, Nusholtz et al. 2007). Additionally, signal analysis of Deceleration Rollover Sled (DRS) test data was presented by Kerrigan et al. (2011) to quantify repeatability of three replicate tests. ISO/TR 16250 discusses signal analysis methods thoroughly and presents a methodology for comparing finite element analysis signals to reference test data signals (ISO, 2013), which also has been published in ISO/TS 18571 (ISO, 2014).

In this study, the ISO method shown in ISO/TR 16250 was adapted to compare test data from repeated DRoTS tests in an attempt to evaluate the repeatability of the test fixture. Assessing repeatability of rollover crash tests by means of how testing equipment can prescribe accurate testing conditions and to produce similar vehicle and occupant kinematics and kinetics was necessary. In addition, it was equally as important to assess these measures against repeatability studies of other, already established and standardized crash tests for comparison. As the National Highway Traffic Safety Administration (NHTSA) has pointed out, repeatability of dynamic rollover tests has not been demonstrated (NHTSA, 2009), thus in evaluating DRoTS repeatability, it was important to draw comparisons to established crash modes to provide for a clear and objective evaluation. Therefore, assessment of test repeatability of the DRoTS was compared to the repeatability of frontal, frontal offset, small overlap, SOI and offset Oblique crash tests.

PREVIOUS STUDIES

The NHTSA had administered the Repeatability Test Program (RTP) to address concerns of repeatability and reproducibility of the 35mph frontal crash test (ISO, 2013). Twelve 1982 Chevrolet Citations were tested at three different test facilities. Variations of the vehicle response

were observed by the different load paths developed through the vehicle frame which ultimately affected dummy response and injury measures. Site-to-site variation existed due to differences in testing procedure and dummy upkeep and thus quantitative variations between facilities could not be calculated. Peak vehicle deformations varied by 15% and ranged from 699mm to 813mm and phase shifts of 10% of the test duration were found.

The Insurance Institute for Highway Safety (IIHS) conducted repeatability of their 40% frontal offset crash test through tests of seven pairs of different vehicle models (Meyerson et al. 1998). Testing procedures were well established and resulted in highly controlled initial conditions. Initial conditions showed maximum difference of 5% overlap for the Hyundai Elantra tests while all other tests showed no difference (Table 3). All impact velocities and test masses varied by 1% or less. Variations in vehicle response were analyzed by comparing peak accelerations (max of 38% or 14G difference in Infinity Q45 pair), visually comparing velocity time histories (similar signals), comparing vehicle deformations by pre- and post-test displacements of single points in the occupant compartment (largest variation in midsize cars was an average intrusion difference of 50%, small cars and passenger vans had average intrusion measures that varied by less than 15%), and visually comparing pre- and post-test vehicle frame rails. Dummy repeatability was evaluated using the calculated Head Injury Criterion (HIC), neck tension, neck extension bending moment, chest deflection, axial femur force, upper and lower tibia index, tibia-femur displacement, lower tibia axial forces, and foot accelerations. Though large variations were seen in dummy injury measures, the IIHS concluded that the overall crashworthiness ratings would not be likely to change categories and thus vehicle performance was repeatable.

The IIHS recently reported repeatability testing of their 25% small overlap frontal crash test using six different vehicles (two tests of five makes and three tests of one make) (Mueller et al. 2013). Initial conditions showed a maximum of 4% difference in mass for Ford Fusion test 4 vs. 12 with most tests below 2% difference (Table 3). All impact velocities were less than 1% difference in all tests and overlap percentage varied at most by 2%. Vehicle accelerations, vehicle deformation measures, dummy kinematics and dummy injury measures were all analyzed again by variations in peaks from time history data and single-value measures. Maximum average intrusion was shown to have a 100% difference for the Volvo S60 pair. Dummy sensor measures mentioned above were also evaluated with the smallest variations resulting in 2-10% error of the Injury Assessment Reference Value (IARV) and the largest variations resulting in 2-75% of the IARV. Small overlap crash tests were “reasonably repeatable” since no changes to IIHS vehicle safety ratings resulted from the variations.

More recently, the NHTSA conducted 20%, 7° small overlap impact (SOI) and 35%, 15° offset Oblique tests using a moving deformable barrier on six tests of the same late model sedan (Saunders et al. 2013). Only nominal test parameters and no initial conditions (test mass, impact velocity, % overlap, and impact angle) were provided however, impact locations were found to be within 25mm of target location for all tests. Saunders et al. (2013) investigated repeatability

of the vehicle using coefficient of variation (CV) of peak vehicle accelerations and point-to-point measurements of deformation from the bumper, door profile, and interior points. Additionally, dummy kinematics and dummy injury measures were analyzed by variations in peaks from time history data and single-value measures. Both vehicle and occupant response were found to have good repeatability in both test modes. Peak vehicle accelerations for both tests showed a maximum of 13.8% variation in the Oblique crash and a maximum of 8.7% variation in SOI. Overall, repeatability of SOI and Oblique crash tests were “equivalent to the repeatability demonstrated in existing tests in the full frontal and offset deformable barrier crash test.”

Unpublished full frontal crashes of model year 2002-2010 vehicles produced for the US market were gathered from the NHTSA crash test database (NHTSA, 2013). Most crash tests of the same vehicle make and model were conducted at different testing facilities. This was seen to have some effect on initial conditions with a maximum of 17% difference in mass for Chevrolet Silverado tests, though most tests were below 6% different (Table 3). All impact velocities were less than 1% different in all tests and all impact angles were recorded as zero.

Kerrigan et al. (2011) presented a detailed assessment of the DRS by testing three replicate vehicles (2002 Ford Explorer) in a simulated rollover. Because of the increased sled speed of V3 test (5%) (Table 4), the vehicle rolled an additional two quarter turns and had 11% more kinetic energy than the other two tests. The authors concluded good repeatability when inertial properties were matched (Kerrigan et al. 2011).

Four rollover tests with two pairs of replicate vehicles (subcompact sedan, tests 1546 and 1519 and compact multi-purpose van (MPV), tests 1662 and 1684) were tested on the DRoTS test fixture. Repeatability was observed based on comparison of touchdown conditions at roof to ground contact and peak measures of sensor data describing vehicle kinematics, kinetics, and deformations.

Table 3: Initial conditions for frontal, frontal offset, small overlap, Oblique, and SOI tests

<i>Small overlap</i>	Test Num.	Mass (kg)	Velocity (kph)	Overlap (%)
2009 Mitsubishi Galant	<i>CF11003</i>	1662	64.1	25
	<i>CF11005</i>	1656	64.3	27
2012 Acura TL	<i>CEN1201</i>	1840	64.2	25
	<i>CEN1214</i>	1863	64.2	25
2012 Acura TSX	<i>CEN1202</i>	1733	64.2	25
	<i>CEN1213</i>	1748	64.2	25
2012 Volvo S60	<i>CF11006</i>	1729	64.2	25
	<i>CF11015</i>	1766	64.2	25
2008 Ford Fusion 02vs04	<i>CF11002</i>	1619	64.3	25
	<i>CF11004</i>	1679	64.3	24
2008 Ford Fusion 02vs12	<i>CF11002</i>	1619	64.3	25
	<i>CF11016</i>	1616	64.4	25
2008 Ford Fusion 04vs12	<i>CF11004</i>	1679	64.3	24
	<i>CF11016</i>	1616	64.4	25

<i>Frontal offset</i>					
1995 Saab900	CF95003	1476	64.5	40	
	CF95017	1489	64.2	40	
1997 Dodge Neon	CF97012	1312	64.0	41	
	CF97019	1308	64.3	41	
1997 Hyundai Elantra	CF97014	1340	64.4	45	
	CF97020	1355	64.8	40	
1997 Infinity Q45	CF97007	1944	64.0	40	
	CF97008	1944	64.5	40	
1996 Pontiac Trans Sport	CF96025	1836	63.4	41	
	CF96026	1852	64.2	41	
<i>Frontal</i>					
2010 Mazda 3	6647	1497	56.5	100	
	6658	1506	56.4	100	
2010 Lexus RX350	6642	2153	56.3	100	
	6643	2163	56.3	100	
2010 Kia Soul	6641	1390	56.6	100	
	6655	1475	56.1	100	
2010 Hyundai Genesis	6759	1744	56.5	100	
	6764	1714	56.5	100	
2010 Honda Insight	6724	1413	56.2	100	
	6729	1428	56.6	100	
2008 Cadillac CTS	6258	2123	56.0	100	
	6271	2124	56.0	100	
2005 Toyota Corolla	5160	1379	56.5	100	
	5388	1566	56.2	100	
2005 Honda Odyssey	5273	2263	56.3	100	
	5714	2388	56.1	100	
2003 Chevrolet Silverado	4472	1918	55.9	100	
	5711	2273	56.2	100	
2002 Toyota Tundra	3915	2401	56.2	100	
	5073	2422	56.3	100	
2002 Dodge Ram	4240	2519	56.5	100	
	5061	2582	56.4	100	
2002 Chevrolet Trailblazer	4244	2348	56.5	100	
	5036	2339	56.7	100	
<i>Oblique</i>					Impact Angle (°)
2011 Chevrolet Cruze	7431	1662	89.7	34.3	345
	7852	1654	90.22	35.5	345
	7851	1650	90.09	35.5	345
<i>SOI</i>					
2011 Chevrolet Cruze	7432	1643	91.04	20.3	353
	7773	1653	90.19	17.8	353
	7867	1654	90.33	17.7	353

Table 4: Initial conditions for DRoTS and DRS tests

Test Numbers	DRoTS				DRS		
	Sedan		MPV		2002 Ford Explorer		
	1519	1546	1662	1684	V1	V2	V3
Pitch Angle (°)*	-12.8	-11.9	-7.7	-7.5	0.0	-0.3	1.5
Roll Angle (°)*	181.0	181.0	-143.2	-146.2	-183.1	-187.3	-196.8
Roll Rate (°/s)*	268	274	-245	-248	-220	-223	-224
Road Speed (m/s)	8.38	8.52	7.54	7.54	3.81	3.65	4.85
Vertical Velocity (m/s)	1.91	1.84	1.67	1.55	3.31	3.21	3.12
Drop Height (mm)	247	234	158	138	478	449	402
Mass As Tested (kg)	1173.9	1181.6	2260.2	2257.6	2324.0	2323.5	2327.0
MOI (kg m ²)	379	378	980	1002	--	--	--

*Pitch and roll angles are expressed in the SAE vehicle coordinate system with negative front-down pitch and positive roll angles in the passenger-side leading direction.

METHODS

Recent studies (International Organization for Standardization (ISO), 2013) have proposed a new methodology for comparing finite element analysis (FEA) simulation signals to experimental test signals. Relative to previous versions (Xu et al. 2000, Gehre et al. 2009), the computation of magnitude and shape errors have changed and a corridor rating, a scoring metric for all four rating methods, and an overall score of the signals have been added. A finalized standard has recently been published (ISO, 2014), however the methodology used in the standard was outlined in ISO/TR 16250.

All test signals follow preprocessing guidelines and threshold values as described in ISO/TR 16250: 10kHz sampling rate, synchronized test signals (ie. $t=0$ has physical meaning of signal characteristics like time of contact/impact is $t=0$), appropriate time interval selected, and filtered signals. This signal analysis methodology was said to have been fully validated by subject matter experts using responses from multiple vehicle passive safety applications (ISO, 2013). Ratings are: Phase rating (E_p), Magnitude rating (E_m), Slope rating (E_s), and CORA corridor rating (E_z). All rating values range from 0 (no correlation) to 1 (perfect correlation) and a weighted average sum of the four ratings yield the final object rating, R ($R = 0.4E_z + 0.2E_p + 0.2E_m + 0.2E_s$). The final objective rating corresponds to a grade, representing the goodness of the correlation between two signals (Poor, $R \leq 0.58$; Fair, $0.58 < R \leq 0.8$; Good, $0.8 < R \leq 0.94$; Excellent, $R > 0.94$). Brief descriptions of the ratings are described below (ISO, 2013):

- Phase error, ε_p was computed as the phase lag between the two signals when maximum cross-correlation (Eq 1) is found within a given time span. Phase rating, E_p (Eq. 2) was computed as a linear regression of the number of phase shifts relative to the maximum allowable time-shift threshold, $\varepsilon_p^* = 0.2$.

$$\rho_L(m) = \frac{\sum_{i=0}^{n-1} [(C(t_{start} + (m+i)\Delta t) - \bar{C}(t)) * (T(t_{start} + i\Delta t) - \bar{T}(t))]}{\sqrt{\sum_{i=0}^{n-1} [(C(t_{start} + (m+i)\Delta t) - \bar{C}(t))^2] * \sum_{i=0}^{n-1} [T(t_{start} + i\Delta t) - \bar{T}(t)]^2}} \quad (Eq. 1)$$

where $\rho_L(m)$ is the left cross correlation value at point m , C and T are the time history test signals, t_{start} is the starting time of the data signals, and Δt is the time step. $\rho_R(m)$ was computed similarly after switching $(m+i)$ with i for test signal C and i with $(m+i)$ for test signal T . The maximum cross correlation value was then used as the phase error, ε_p and the phase score can be computer as:

$$E_p = \frac{\varepsilon_p^* * N - \varepsilon_p}{\varepsilon_p^* * N} \quad for \quad \varepsilon_p \leq \varepsilon_p^* * N \quad (Eq. 2)$$

where N is the total number of sample points.

- Magnitude error, ε_{mag} was computed as the difference in amplitude between test signals after a dynamic time warping algorithm (minimization of error in phase and slope) was applied (Eq. 3). Magnitude rating, E_m (Eq. 5) was calculated as a linear regression of the magnitude error relative to the maximum allowable magnitude error, $\varepsilon_M^* = 0.5$.

$$d(i, j) = (C^{ts}(i) - T^{ts}(j))^2 \quad (Eq. 3)$$

where $d(i, j)$ is the cost function and C^{ts} and T^{ts} are the time shifted test signals. Once cost function was built a path of lowest cost was associated to the test signals creating time shifted and warped test signals, C^{ts+w} and T^{ts+w} . The magnitude error was then computed (Eq. 4) which then led to the computation of the magnitude score (Eq. 5):

$$\varepsilon_{mag} = \frac{\|C^{ts+w} - T^{ts+w}\|_1}{\|T^{ts+w}\|_1} \quad (Eq. 4) \quad E_m = \frac{\varepsilon_m^* - \varepsilon_{mag}}{\varepsilon_m^*} \quad for \quad \varepsilon_{mag} \leq \varepsilon_m^* \quad (Eq. 5)$$

- Slope error, ε_{slope} was computed as the difference in slope between signals relative to the test curve when no time lag exists (Eq 6). Slope values were calculated by average slopes at each point across a 1ms time interval for each signal, creating time shifted and derivative test signals, C^{ts+d} and T^{ts+d} . Slope rating, E_s (Eq. 7) was calculated as a linear regression of the slope error relative to the maximum allowable slope error, $\varepsilon_s^* = 2$.

$$\varepsilon_{slope} = \frac{\|C^{ts+d} - T^{ts+d}\|_1}{\|T^{ts+d}\|_1} \quad (Eq. 6) \quad E_s = \frac{\varepsilon_s^* - \varepsilon_{slope}}{\varepsilon_s^*} \quad for \quad \varepsilon_{slope} \leq \varepsilon_s^* \quad (Eq. 7)$$

- CORA corridor rating, E_z (Eq. 9) was computed as the average of all single time step ratings (Eq. 8). The corridor rating at time, t is the squared regression of the difference of the two signals relative to the corridor width.

$$Z(t) = \begin{cases} 1 & \text{if } |T(t) - C(t)| < \delta_i \\ \left(\frac{\delta_o - |T(t) - C(t)|}{\delta_o - \delta_i} \right)^2 & \\ 0 & \text{if } |T(t) - C(t)| > \delta_o \end{cases} \quad (Eq. 8) \quad E_Z = \frac{\sum_{t=t_{start}}^{t_{end}} Z(t)}{N} \quad (Eq. 9)$$

where δ_o is the absolute half width of the outer corridor defined as

$\delta_o = 0.5 * \max(|\min(T)|, |\max(T)|)$ and δ_i is the absolute half width of the inner corridor defined as $\delta_i = 0.05 * \max(|\min(T)|, |\max(T)|)$.

Following this methodology custom code was written in MATLAB and verified to provide a means for quantifying repeatability of test signals as opposed to simulation data relative to test data. Verification of code was completed by digitizing test cases presented in ISO/TR 16250 and comparing individual ratings.

Signal analysis comparisons were completed for frontal, frontal offset, small overlap, SOI, Oblique, DRoTS, and DRS repeated test data. Test data of the frontal offset and some of the small overlap tests were publicly available from the IIHS techdata webpage (IIHS, 2013) while the remaining small overlap test data was collected through personal communication with the IIHS (Mueller et al. 2013). Frontal, SOI, and Oblique test data were publicly available from the NHTSA crash test database (NHTSA 2013). Rollover tests were completed by the authors of this study and published either previously (DRS) or concurrently (DRoTS). Signal analysis was performed on all available time history data related to vehicle acceleration, vehicle deformation, and vehicle boundary conditions (where applicable). The time span selected for signal analysis depended on crash type and was based on impact duration: 0.155s for frontal, SOI, and Oblique tests, 0.205s for small overlap tests, 0.255s for frontal offset tests, 0.305s for DRoTS tests, and 2.005 for DRS tests.

RESULTS

Coordinate systems follow SAE standard J670 for vehicle coordinate system (+X from rear to front of vehicle, +Y from driver to passenger, +Z from roof to base of vehicle). Global coordinates follow +X' as direction of road/vehicle travel, +Z' as direction of gravity, and +Y' as the cross product of Z' with X'. For the purpose of this report and for direct comparisons between tests, global Y' direction from DRS data was referred to as global X', and global X' direction from DRS data was referred to as global Y' (neglecting sign since values presented were absolute).

Small Overlap Impact (SOI) and Oblique Crashes

Compared to vehicle Y acceleration and floorpan displacement (grade was fair or poor), vehicle X acceleration (grade was good) showed the best repeatability for all pairs of tests (Table 5, Appendix C).

Table 5: Overall test signal ratings (R) and grades for SOI and Oblique crash tests

C.Cruze Oblique	7431vs7852	7431vs7851	7852vs7851
Veh. CG X Accel	0.817 ***	0.842 ***	0.858 ***
Veh. CG Y Accel	0.635 **	0.667 **	0.523 *
Floorpan- Right Front Disp.	0.247 *	0.095 *	0.348 *
C.Cruze SOI	7432vs.7773	7432vs.7867	7773vs.7867
Veh. CG X Accel	0.758 **	0.797 **	0.912 ***
Veh. CG Y Accel	0.441 *	0.568 *	0.559 *
Floorpan- Right Front Disp.	0.014 *	0.292 *	0.014 *

Signal grades: * = poor, **=fair, ***=good, ****=excellent

Small Overlap

Selected accelerations for all vehicle types received a fair grade with the exception of the resultant acceleration of Acura TL (good) and the Volvo S60 (Table 6, Appendix D), which received poor grades for all accelerations.

Table 6: Overall test signal ratings (R) and grades for small overlap tests

	2009 Mit. Galant	2012 Acura TL	2012 Acura TSX	2012 Volvo S60	2008 Ford Fusion 02vs04	2008 Ford Fusion 02vs12	2008 Ford Fusion 04vs12
Veh. CG X Accel.	0.781 **	0.770 **	0.740 **	0.460 *	0.783 **	0.785 **	0.725 **
Veh. CG Y Accel.	0.767 **	0.719 **	0.726 **	0.469 *	0.752 **	0.745 **	0.729 **
Veh. Resultant Accel.	0.784 **	0.818 ***	0.800 **	0.324 *	0.794 **	0.771 **	0.739 **

Signal grades: * = poor, **=fair, ***=good, ****=excellent

Frontal Offset

Overall, vehicle accelerations were generally close to the boundary between fair and good grades (Table 7, Appendix E).

Table 7: Overall test signal ratings (R) and grades for frontal offset crash tests.

	1995 Saab 900	1997 Dodge Neon	1997 Hyundai Elantra	1997 Infiniti Q45	1996 Pontiac Trans Sport
Veh. CG X Accel	0.825 ***	0.787 **	0.760 **	0.832 ***	0.820 ***
Veh. CG Y Accel	0.688 **	0.809 ***	0.818 ***	0.693 **	0.662 **
Veh. Resultant Accel	0.864 ***	0.785 **	0.776 **	0.803 ***	0.811 ***

Signal grades: * = poor, **=fair, ***=good, ****=excellent

Frontal

The summed total barrier force and accelerations showed strong correlations; all grades were good for barrier force while accelerations were split evenly between good and fair (Table 8). Nearly all vehicle Z accelerations showed poor repeatability since vehicle Z acceleration has very low magnitude in a frontal crash. All scoring metrics and errors for all tested vehicles were recorded (Appendix F).

Table 8: Overall test signal ratings (R) and grades for frontal crash tests

	Seat-Left Rear X	Seat-Right Rear X	Seat-Left Rear Z	Seat-Right Rear Z	Sum Total Force
2010 Mazda 3	0.829 ***	0.825 ***	0.361 *	0.482 *	0.822 ***
2010 Lexus RX350	0.881 ***	0.872 ***	0.423 *	0.429 *	0.882 ***
2010 Kia Soul	0.746 **	0.863 ***	0.497 *	0.506 *	0.879 ***
2010 Hyundai Genesis	0.761 **	0.802 ***	0.315 **	0.557 *	0.994 ****
2010 Honda Insight	0.765 **	0.792 **	0.712 **	0.722 **	0.886 ***
2008 Cadillac CTS	0.792 **	0.895 ***	0.626 *	0.607 *	0.92 ***
2005 Toyota Corolla	0.818 ***	0.839 ***	0.479 *	0.430 *	0.883 ***
2005 Honda Odyssey	0.734 **	0.829 ***	--	--	0.890 ***
2003 Chevrolet Silverado	0.815 ***	0.776 **	--	--	0.850 ***
2002 Toyota Tundra	0.865 ***	0.858 ***	--	--	0.872 ***
2002 Dodge Ram	0.731 **	0.768 **	--	--	0.845 ***
2002 Chevrolet Trailblazer	0.874 ***	0.862 ***	--	--	0.891 ***

Signal grades: * = poor, **=fair, ***=good, ****=excellent

Rollover

Since V3 in the DRS test had 11% more kinetic energy than V1 or V2, the difference in vehicle performance was reflected in ratings between pairs of tests that involve V3 (Table 9); vehicle X data signals between V1 vs. V2 were higher rated since the 5% increase in sled velocity was transferred to rotational energy which accounts for the differences when comparing signals to V3. All other correlations made with V3 were not appreciably worse than they were in the V1 vs V2 comparison. All rating metrics were recorded (Appendix H).

Signal analysis was performed on vehicle kinematics, deformations, and forces for the DRoTS tests (Table 9, Figure 14) and all rating metrics were recorded (Appendix G). MPV tests showed better repeatability across vehicle X data signals as expected since vehicle fixation was an issue in the sedan tests. However, some global components of the sedan tests had higher grades than the van tests.

Table 9: Overall test signal ratings (R) and grades for DRoTS and DRS rollover crash

	1546 vs. 1519	1662 vs. 1684	Ford Explorer V1 vs V2	Ford Explorer V1 vs V3	Ford Explorer V2 vs V3
Veh. X Ang. Accel.	0.502*	0.553*	0.657**	0.615**	0.592**
Veh. Y Ang. Accel.	0.582**	0.475*	0.630**	0.637**	0.522*
Veh. Z Ang. Accel.	0.564*	0.545*	0.543*	0.619**	0.556*
Veh. X Ang. Vel.	0.606**	0.743**	0.769**	0.489*	0.432*
Veh. Y Ang. Vel.	0.670**	0.600**	0.537*	0.655**	0.428*
Veh. Z Ang. Vel.	0.649**	0.631**	0.690**	0.442*	0.629**
Veh. X Ang. Disp.	0.823***	0.988****	0.986****	0.543*	0.460*
Veh. Y Ang. Disp.	0.875***	0.865***	0.559*	0.122*	0.116*
Veh. Z Ang. Disp.	0.953****	0.939***	0.380*	0.384*	0.353*
Global X CG Accel.	0.608**	0.595**	0.651**	0.626**	0.582**
Global Y CG Accel.	0.690**	0.516*	0.647**	0.618**	0.613**
Global Z CG Accel.	0.765**	0.600**	0.634**	0.627**	0.584**
Global X CG Vel.	0.766**	0.518*	0.936***	0.882***	0.853***
Global Y CG Vel.	0.373*	0.684**	0.291*	0.225*	0.711**
Global Z CG Vel.	0.885***	0.853***	0.843***	0.705**	0.658**
Global X CG Disp.	0.662**	0.246*	0.993****	0.857***	0.799**
Global Y CG Disp.	0.361*	0.536*	0.080*	0.092*	0.776**
Global Z CG Disp.	0.967****	0.957****	0.862***	0.833***	0.887***
Total Vertical Load	0.842***	0.821***	--	--	--
Road Velocity	0.888***	0.941****	--	--	--

Signal grades: * = poor, **=fair, ***=good, ****=excellent

Examples of Ratings for Deformation, Reaction Load, and Acceleration Signals

The range of ratings for deformation, reaction force and accelerations are shown in Figure 11 - Figure 13. Examples of each of the ratings are shown in Figure 11 left and Figure 13 left (poor), Figure 13 middle (fair), Figure 11 middle Figure 12 all Figure 13 right (good), and Figure 11 right (excellent).

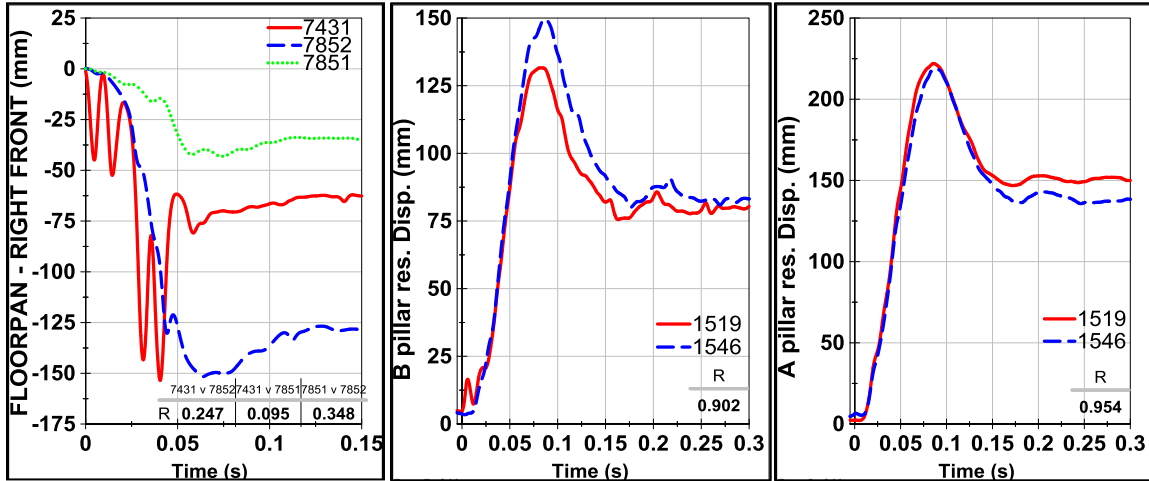


Figure 11: Examples of vehicle resultant deformation measures and their respective correlation values. From left to right: Chevy Cruze SOI tests (poor grade), DRoTS Sedan tests (good grade), and DRoTS Sedan tests (excellent grade)

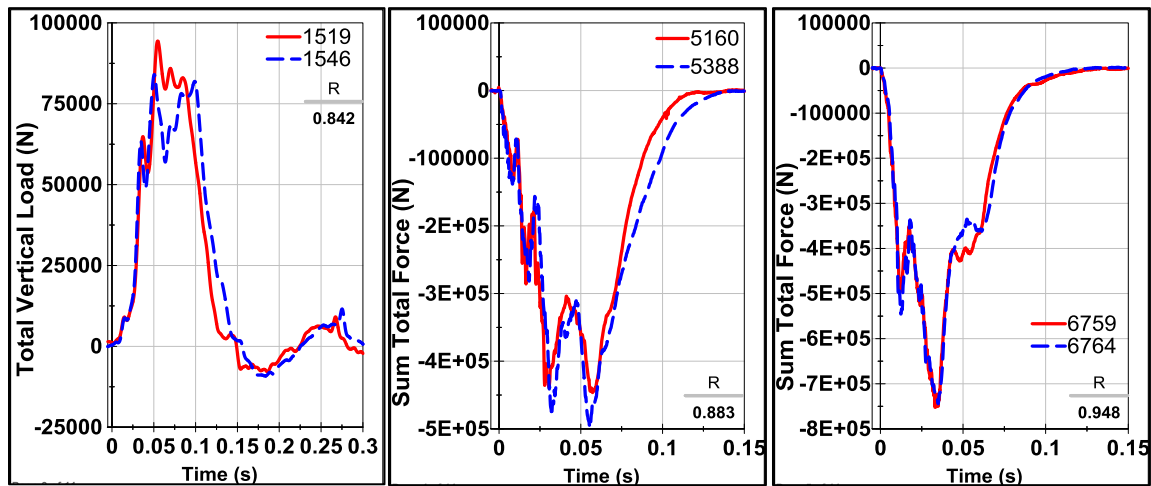


Figure 12: Examples of total reaction load measures and their respective correlation values. From left to right: DRoTS Sedan tests (good grade), Frontal Toyota Corolla tests (good grade), and Frontal Hyundai Genesis tests (good grade)

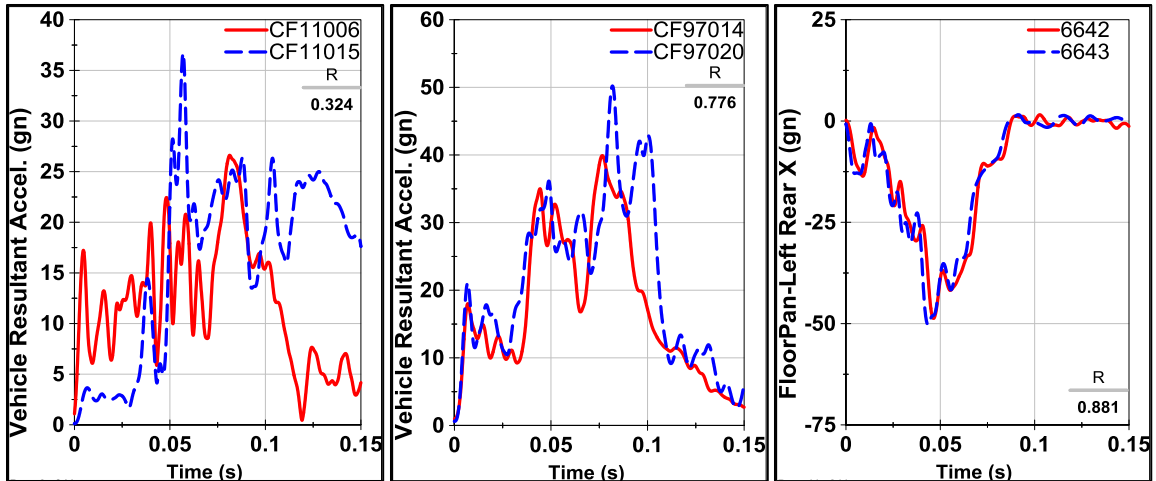


Figure 13: Examples of vehicle dominant acceleration signals and their respective correlation values. From left to right: Small Overlap Volvo S60 (poor grade), Frontal Offset Hyundai Elantra tests (fair grade), and Frontal Lexus RX350 tests (good grade)

DISCUSSION

An overall grading system was developed by the authors of ISO/TR 16250 to characterize the correlation of paired signals based on case studies they developed. Their rating metric was said to have been “fully validated using response from multiple vehicle passive safety applications,” however this was based on the opinion of “subject matter experts” who decided what the sliding scale and weighting factors should be (ISO, 2013). The sliding scale can only be applied to the overall rating (R) of signals that have been preprocessed according to ISO and have been analyzed using the weighting factors and maximum error values defined by ISO. Any change required a “revision of the grade’s thresholds, (ISO, 2013).” The grading scale was described as follows: excellent means the “characteristics of the reference signal are captured almost perfectly,” good means the “characteristics of the reference signal are captured pretty good, but there are noticeable differences between both signals,” fair means the “characteristics of the reference signal are basically captured, but there are significant differences between both signals,” and poor means “there is almost no correlation between both signals,” (ISO, 2013).

The validation of ISO’s method included crash impulses for testing passive safety systems, similar to the kinds of responses for the crash tests evaluated in this paper. Thus, the overall rating and corresponding grade defined by ISO were used to evaluate repeatability of the DRoTS test fixture without changing ISO specified values. Since all individual ratings needed to be determined to determine R, the individual ratings are provided for the reader in the Appendices.

To provide a basis to compare all crash tests against one another, acceleration data were resolved such that each dominant acceleration signal was used and thereby eliminated noisy low rated signals. In other words, vehicle X acceleration was the only signal used for the frontal crash tests, all other non-rollover tests used the resultant of the vehicle X and Y accelerations, and

rollover tests used the resultant of the global X' and Z' accelerations to yield the dominant accelerations. For DRoTS, global X' accelerations were used because of similar magnitudes ($\pm 5g$'s) to global Z' accelerations (+2.5, -7.5 g's), although global X' accelerations are not representative of the vehicle kinematics (DRoTS restricts vehicle motion in this direction), it was indicative of the deformation of the vehicle captured by the accelerometers which still would be important to consider for assessing repeatability of replicate tests.

Frontal Offset, Small Overlap, SOI and Oblique Crashes

Frontal offset signal analysis of vehicles tested by Meyerson et al. (1998) had overall ratings near the boundary of fair and good grades. Vehicle performance presented by Meyerson et al. (1998) showed substantial variations between repeated tests while peak accelerations were said to be similar until accelerometer mounting locations were compromised, which was in agreement with the signal grades.

Mueller et al. (2013) reported vehicle crash test ratings of select tested vehicles which showed that overall ratings (based on component ratings of dummy injury measures, dummy kinematics and restraints, and vehicle structural performance) were similar between those paired tests: Volvo S60 and Acura TL received good ratings, and Acura TSX received marginal ratings. Since the overall ratings did not change across paired tests, the authors concluded that the tests were repeatable. However, signal analysis showed fair grades in accelerations for all pairs except for Volvo S60 (poor grades) (Table 6) indicating a lack of repeatability in the vehicle kinematics despite the authors' conclusions.

Saunders et al. (2013) reported displacement time histories of the right rear sill for all tested vehicles in the SOI and Oblique crashes and all paired signals resulted in a poor grade between test signals (Table 5). Displacements recorded in the Oblique tests also showed substantial rebound: test 7431 rebounded to less than half the peak displacement (153mm to 71mm) within 30ms which did not happen in the other tests (Figure 11). Despite displacement time histories showing nearly no correlation, vehicle X CG acceleration ratings show much better correlation and were in agreement with the subjective conclusion that repeatability was good Saunders et al. (2013) reported. However, y-acceleration ratings showed mostly poor grades.

Rollover

Since predominant rotation is about the vehicle X axis and since DRoTS prevents global Z' rotations, the dominant data signals chosen to be evaluated were angular velocity about the vehicle local X and Y axes (roll and pitch rates), angular displacement about the vehicle local X

axis, acceleration in the global X' & Z' directions and their resultant, road reaction force in the global Z' direction and resultant pillar displacements.

For both paired DRoTS tests, local X angular velocity and global Z' acceleration received fair grades. In the case of angular acceleration about the local X axis, the signals received poor grades. This was due, in part, because angular acceleration was calculated from taking a derivative of the angular velocity data and noise was substantially introduced in the signal. The presence of noise has been shown to have a negative effect on rating methods (ISO, 2013) since the maximum cross correlation value may cause a non-representative phase offset, which in turn will cause large magnitude and slope errors. Even if phase error remained unchanged from the added noise, magnitude and slope ratings would be affected since the added peaks would cause large magnitude differences and the numerical derivative would have even more added noise. Additionally, the corridor rating would be negatively impacted by noise since the signal may constantly go in and out of the specified corridor widths.

Phase errors of selected channels for tests 1519 vs. 1546 were less than 5ms with the exception of local X angular velocity, which indicated the recorded response resulted from the same physical impact and the vehicle responded similarly throughout the impact. The large phase error in local X angular velocity was attributed to the shift in roll axis after impact when the vehicle in test 1519 deviated from the roll rates measured in the other test, as described in the previous study. This resulted in a larger phase error, which ultimately affected the remaining scoring metrics.

Despite changes in hardware of the DRoTS test equipment aimed at improving test repeatability, signal analysis ratings of tests 1662 vs 1684 did not get substantially better (Table 9, Figure 14). However, it was hypothesized that the lower ratings resulted from a 20 kg m² increase in moment of inertia (MOI) and 53.5mm shift in center-of-gravity (CG) location.

In nearly every kinematic result, DRoTS tests showed, on average, a higher level of repeatability than the DRS tests (Figure 14). Thus, DRoTS using this rating technique, can be said to have at least as good or better repeatability than DRS. However, global X' velocity and displacement ratings were significantly lower because the DRoTS system held the vehicle in a vertical plane such that the vehicle could not translate in the global X' direction (Kerrigan et al. 2011 SAE) which caused accelerometer readings to show high oscillations and ultimately affected the overall rating.

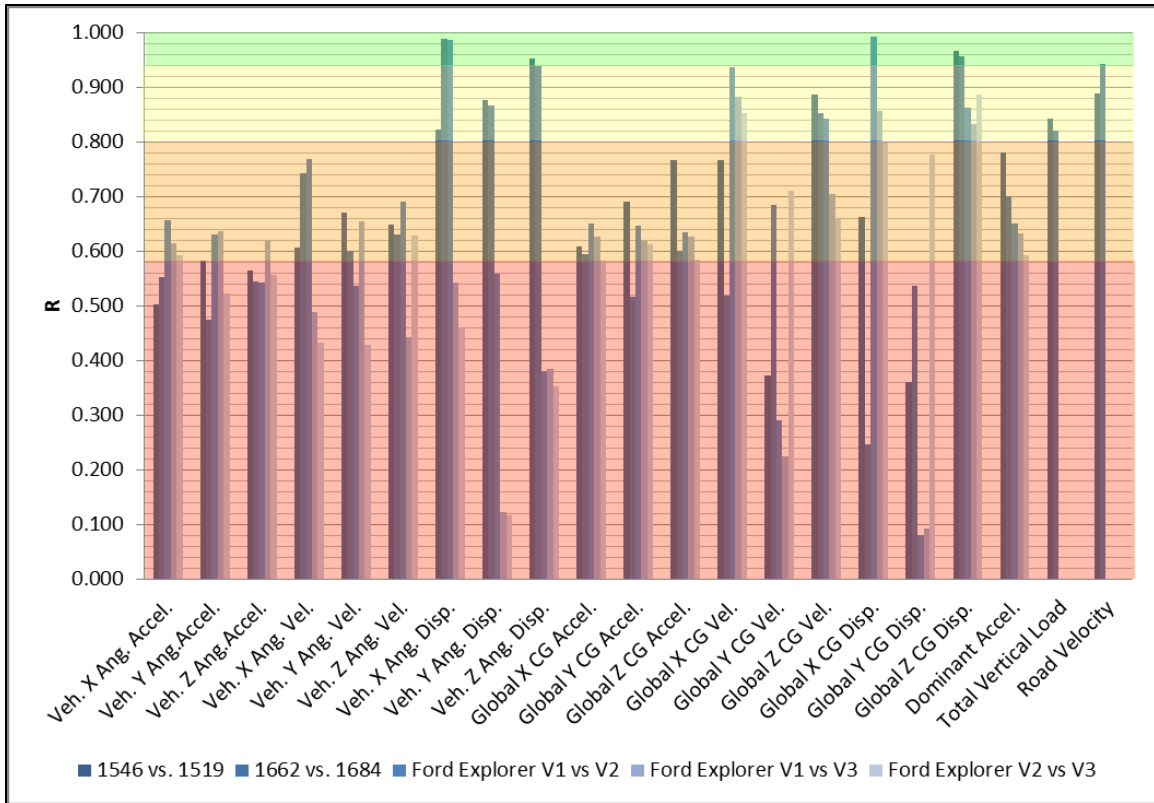


Figure 14: Overall ratings for kinematic and force signals from rollover crash tests

Repeatability Comparison of Crash Tests

Using the dominant metrics previously defined, the ranking of the repeatability of each crash test was compared using the average R value for the dominant accelerations. The resulting repeatability ranking was (from most repeatable to least): 1) Frontal Offset (0.808), 2) Frontal (0.801), 3) Oblique (0.794), 4) SOI (0.778), 5) DRoTS (0.740), 6) Small Overlap (0.719), and 7) DRS (0.625) (Figure 15). This result agrees with the findings presented by Saunders et al. (2013) that indicated the repeatability of the SOI crash was similar to that of the Oblique crash. Using only one single acceleration direction for each test (vehicle X acceleration for non-rollover tests and global Z' acceleration for rollover tests) the resulting rankings were: 1) Oblique (0.839), 2) SOI (0.822), 3) Frontal Offset (0.805), 4) Frontal (0.801), 5) Small Overlap (0.721), 6) DRoTS (0.683), and 7) DRS (0.615). Comparison and variation of the average ratings for each crash test type can be found in Appendix I.

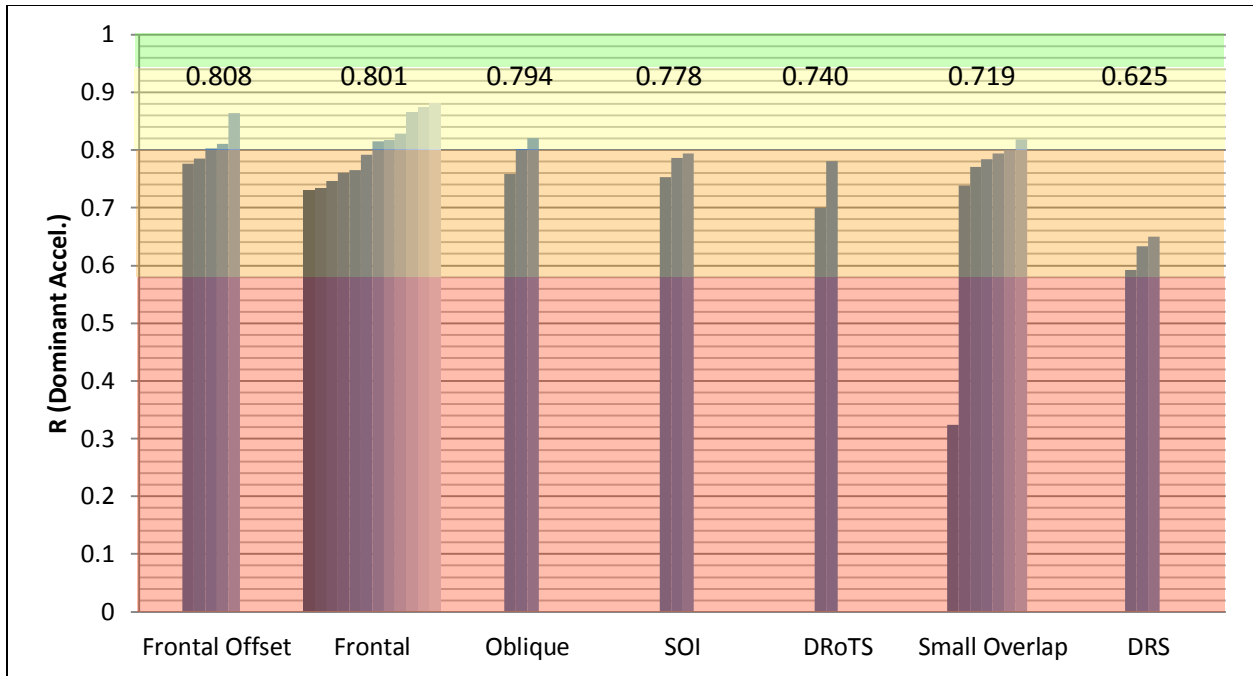


Figure 15: Dominant acceleration ratings for all crash tests, average scores shown above respective crash test

This ranking does not support the conclusions made by Mueller et al. (2013), who reported that vehicle acceleration in the small overlap test was more repeatable than the frontal offset test conducted by Meyerson et al. (1998). Based on the average dominant acceleration, frontal offset showed the highest level of repeatability of all crash tests. Even if the Volvo S60 was not included in the assessment for the small overlap tests (as manufacturing of the vehicle was indicated by Mueller et al. (2013) to be the main cause of variation and not the testing equipment/procedure), the frontal offset still ranks higher.

Despite the large discrepancy in vehicle acceleration (Figure 13) of the Volvo S60 tests, both tests resulted in the same IIHS crash ratings for structure, restraints and kinematics, and dummy injury measures which lead to Mueller's conclusion that the tests were repeatable. The same crash rating was awarded because no ratings are dependent on the vehicle kinematic response, rather the structure rating was determined from intrusion of structural members and all other ratings were dependent on dummy kinematics and injury measures. This may be an indicator that acceleration may not be the best evaluation for repeatability of dummy kinematics and injury measures.

All data signals analyzed and separated in terms of signal type revealed that, on average, force data showed higher correlations than acceleration or deformation data (Figure 16). Ratings for the dominant acceleration ranged from 0.324 (Small Overlap: Volvo S60) to 0.881 (Frontal: Lexus RX350) across all analyzed tests, total force ranged from 0.821 (DRoTS: 1662 vs 1684) to 0.948 (Frontal: Hyundai Genesis), and displacement data ranged from 0.014 (7432 vs. 7773) to 0.954 (1519 vs 1546) for Oblique, SOI, and DRoTS tests. While overall DRoTS scores were

lower than other crash tests, force repeatability was on par with Frontal crash test (all grades were good) and deformation repeatability was highest overall. And deformations may be the, or one of the, most important factors in rollover testing due to its relationship to occupant injury (Austin, 2010; Strashny, 2007)

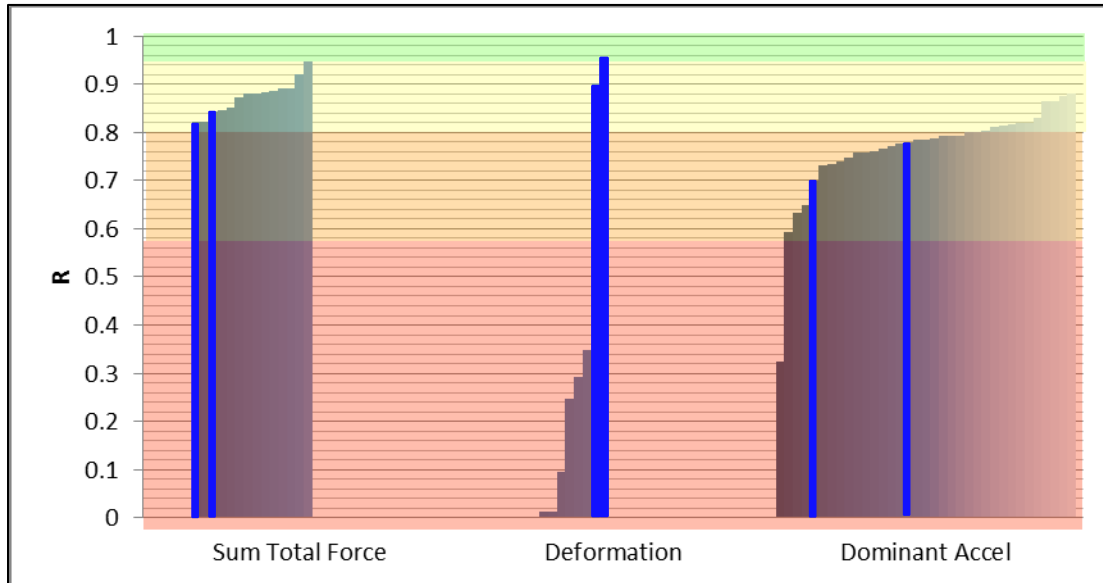


Figure 16: Overall ratings for varied signal types encountered (highlighted bars indicate DRS tests)

CONCLUSION

This study aimed to examine the repeatability of vehicle responses across a variety of vehicle crash tests, using the objective rating metrics described by ISO, in an effort to evaluate the repeatability of a new rollover test method: DRS. Repeatability was evaluated and compared across crash tests using vehicle accelerations, deformations, and impact forces.

The DRS test fixture was found to be more repeatable than the DRS in nearly every kinematic response of the vehicles tested. On average, overall ratings indicated greater repeatability in angular and linear acceleration, velocity, and displacements with the exception of global X' (road direction of travel) velocity and displacement. As concluded by Kerrigan et al. (2011), the DRS was highly repeatable when inertial properties were very similar, therefore the DRS can be said to have as good or better repeatability than the DRS.

Frontal crash tests showed good repeatability in acceleration and force measures as expected since they have been long studied and are only concerned with one primary direction of travel. All other crash tests averaged fair repeatability in dominant acceleration except for Frontal Offset, which averaged good repeatability. Deformation measures of SOI and Oblique tests showed no correlation.

When comparing all crash tests with dominant accelerations, DRoTS ranked 5th of the 7 tests. The crash tests ranked as: 1) Frontal Offset, 2) Frontal, 3) Oblique, 4) SOI, 5) DRoTS, 6) Small Overlap, 7) DRS. When comparing tests with force data, DRoTS was as good as Frontal crash tests. When comparing tests with deformation data, DRoTS was better than all other tests. Thus, the DRoTS was shown to have as good or better repeatability than other crash tests used in regulatory and consumer testing.

LIMITATIONS OF THE ISO METHOD

This was not an all-inclusive study on objective rating methods to assess repeatability. Rather this study examined the use of a method proposed by ISO to quantify the level of similarity between time history signals as a way to evaluate repeatability. The method proposed by ISO was adopted to objectively assess repeatability of replicate tests rather than between test and simulation data, as the ISO method was originally intended. Without changing any parameters provided by ISO, similar conclusions of signal correlations described by ISO can be drawn in this study. However, these parameters would not be ideal for assessing full scale vehicle crash tests from my understanding of the calculations even though subject matter experts have claimed to have “validated” test-simulation data signal correlations with passive safety system sled tests. The actual validation of these signals has been inferred and the ISO does not provide any clear description as to why the specified parameters were used. For example, the weighted average of the scoring metrics was not discussed: the CORA corridor method was weighted heavier than the magnitude, slope and phase metrics while magnitude, slope, and phase metrics were all equally weighted. In addition each error calculation used a maximum allowable error ($\varepsilon_p^* = 0.2$, $\varepsilon_M^* = 0.5$, and $\varepsilon_s^* = 2$) to generate each scoring metric and a sliding scale (Poor, $R \leq 0.58$; Fair, $0.58 < R \leq 0.8$; Good, $0.8 < R \leq 0.94$; Excellent, $R > 0.94$) was predefined. The maximum errors and boundaries of the sliding scale were not discussed or justified by the ISO (2013), which makes evaluations of the choices made by the ISO, and proposition of other choices, difficult if not impossible.

Since the weighting factors were “validated” based on test-to-simulation results of passive safety systems from dummy kinematic responses, these weights may not be appropriate for analyzing repeatability of test-to-test vehicle response data. Ideally, the DRoTS will be used to assess injury in rollover crashes using dummy responses similar to all crash tests conducted by NHTSA to evaluate the risk of injury to occupants. Thus, the weighting factors of this method will need to be chosen justifiably such that the overall repeatability value would clearly discriminate between injurious and non-injurious cases. By conducting replicate tests which report the same level of injury from dummy measures, the weighting factors can be adjusted to indicate a high level of repeatability and if the replicate tests measure different levels of injury the overall repeatability rating will indicate a low correlation value. Additionally, if a baseline rollover test is picked and the input parameters are varied slightly for subsequent tests, different levels of injury will be observed, which will also be captured in the overall repeatability rating when the weighting factors are adjusted appropriately. The issue with developing some baseline rollover case is determining how severe the rollover parameters should be. Increasing the severity of the roll conditions would expectedly increasing discrepancies to smaller variations in input conditions and in turn would affect the repeatability rating.

Limitations of the studies presented in this thesis also have an effect on the outcome of the ISO metric. Only two rollover conditions were studied, one set matched a real world rollover crash scenario and the other set used roll conditions of mild severity based on rollover tests reported by Funk et al. (2012). No set standard rollover test exists so choosing initial conditions for a rollover crash test changes the severity of the impact. In addition, this study inherently assumed that the test vehicles were identical since the repeatability assessment of the DRoTS fixture was based on the performance of vehicles tested. Vehicles are complex systems with many assemblies of individual components and variation may arise from physical differences in component design, differences in material properties, or in differences of joined connections such as welds or bolted/screwed attachments. New and late model vehicles were used in this study to reduce variability but manufacturing differences can still exist and cannot easily be distinguished from variation caused by the test fixture during testing and can therefore affect the vehicle response and overall repeatability assessment.

For use of these metrics in evaluating crash test repeatability, I believe the phase metric should be eliminated because there was no need to time shift data curves of two tests relative to each other that have been conducted to explicitly simulate one another. That is, the subsequent test replicates that of its predecessor and input parameters are nearly identical, thus allowing for a possibly arbitrary time shift removes any physical meaning of the test time spectrum from the comparison. Time equal to zero typically represents an event has occurred at that instant and if a time shift was forced to maximize cross correlation values then the zero point could be arbitrarily shifted. Additionally, most data signals received phase scores greater than 0.900, and the few that did receive lower scores were drastically lower because the signals had lower magnitude, which affects the interpretation of time zero. However, when evaluating dummy responses, the phase offset may be useful if delay in dummy motion exists. Therefore, correcting the phase offset before comparing magnitude and slope characteristics of dummy measures will increase the likelihood of comparing similar levels in each of these measures.

The other key issue with the ISO method was the lack of ability to compare across multiple tests or simulations. Repeatability can only be measured between two tests or one test and one simulation. This is helpful when validating simulation studies to a single experimental test, but if there were multiple tests with similar test articles, one test may have to be arbitrarily chosen as the baseline to which other tests are compared. Otherwise, attempting to average output signals to create a possible baseline would destroy any type of meaning of the signals and would be highly sensitive to phase offsets. Hovenga et al. (2005) developed a method for looking at single value comparisons, time history signal comparisons and a method to incorporate all time history signals from multiple tests into a scoring metric based on signal type (i.e. acceleration, force, deformation, ...) and a final score for all the groups of data comparisons. This approach would be more meaningful when sample size is greater than two and a more encompassing conclusion could be drawn about all tests compared. However, there would be an issue if there were any

tests that look drastically different from the other tests, as in an outlier, which would compromise the overall comparison and would need to be evaluated separately against the other tests. In addition, a study of Hovenga's method showed that at 1ms phase offset of a reference curve compared against itself had a significant reduction in Hovenga's shape correlation (21%), concluding that curves with steep slopes and curves oscillating around zero would cause this reduction (Eriksson et al. 2009). For these reasons, Hovenga's method was not used here. If the ISO method could further expand to evaluate groups of data sets, the ISO method would become a more powerful tool and would help distinguish variation in repeatability studies such as variation across test subjects, equipment setup, and sensor readings. All-in-all, the ISO method was a good approach for evaluating repeatability. Despite the drawbacks mentioned above, the ISO method was a valuable tool for evaluating repeatability and should be used in future repeatability studies.

THESIS CONCLUSIONS

This thesis evaluated repeatability of the DRoTS fixture by comparing touchdown conditions of replicate tests and by comparing signals of vehicle kinematics, kinetics, and deformations measures. The DRoTS fixture is capable of prescribing repeatable touchdown conditions: all touchdown conditions (roll and pitch angle, roll rate, drop height, vertical velocity, and road speed) were less than 8% different between replicate tests with the exception of drop height for the compact multi-purpose van (MPV) tests (14%, 20mm difference). Vehicle kinematics (roll rate, road speed, roll and pitch angle, global Z' acceleration, and global Z' velocity) were similar throughout the impact, however differences were seen in the sedan tests because of a vehicle fixation problem and differences were seen in the MPV tests due to an increase in reaction forces during leading side impact likely caused by disparities in roll angle (3° difference) and mass properties (2.2% in MOI, 53.5mm difference in CG location). Despite those issues, kinetic and deformation measures showed a high degree of repeatability which is necessary for assessing injury risk in rollover as roof strength positively correlates with injury risk (Brumbelow, 2009). The deviation from a repeatable response as a result of differences in inertial properties was also observed by Kerrigan et al. (2011) when using the DRS to conduct a repeatability study. Therefore, when the inertial properties are very similar, the DRoTS system can produce repeatable dynamic rollover tests.

Though the first study presented repeatability of the time history data, results comparing time history signals were subjective analyses, similar to previous repeatability studies of crash tests. Thus, in the second study an objective rating method proposed by ISO (2013) was used to correlate data signals of replicate tests by means of quantifying signal characteristics and providing an overall rating of correlation. Ratings of vehicle kinematics, kinetics and deformations were compared across standardized crash tests and dynamic roll over systems (Frontal, frontal offset, small overlap, SOI, Oblique, DRoTS, and DRS). Average overall ratings of vehicle kinematics for the DRoTS replicate tests were higher (demonstrating greater repeatability) in nearly every aspect compared to the DRS replicate tests. Ratings of dynamic deformation measures were significantly higher in the DRoTS tests when compared to SOI and oblique crash tests. Ratings of the summed vertical loads in the DRoTS tests were slightly lower than the ratings of summed barrier forces of frontal crashes but all reaction force signals received good repeatability grades. When the average dominant acceleration rating was used to compare across all presented crash scenarios, the DRoTS ranked 5th of 7 and thus, the DRoTS fixture can be concluded to be as repeatable as other crash tests when comparing the vehicle response.

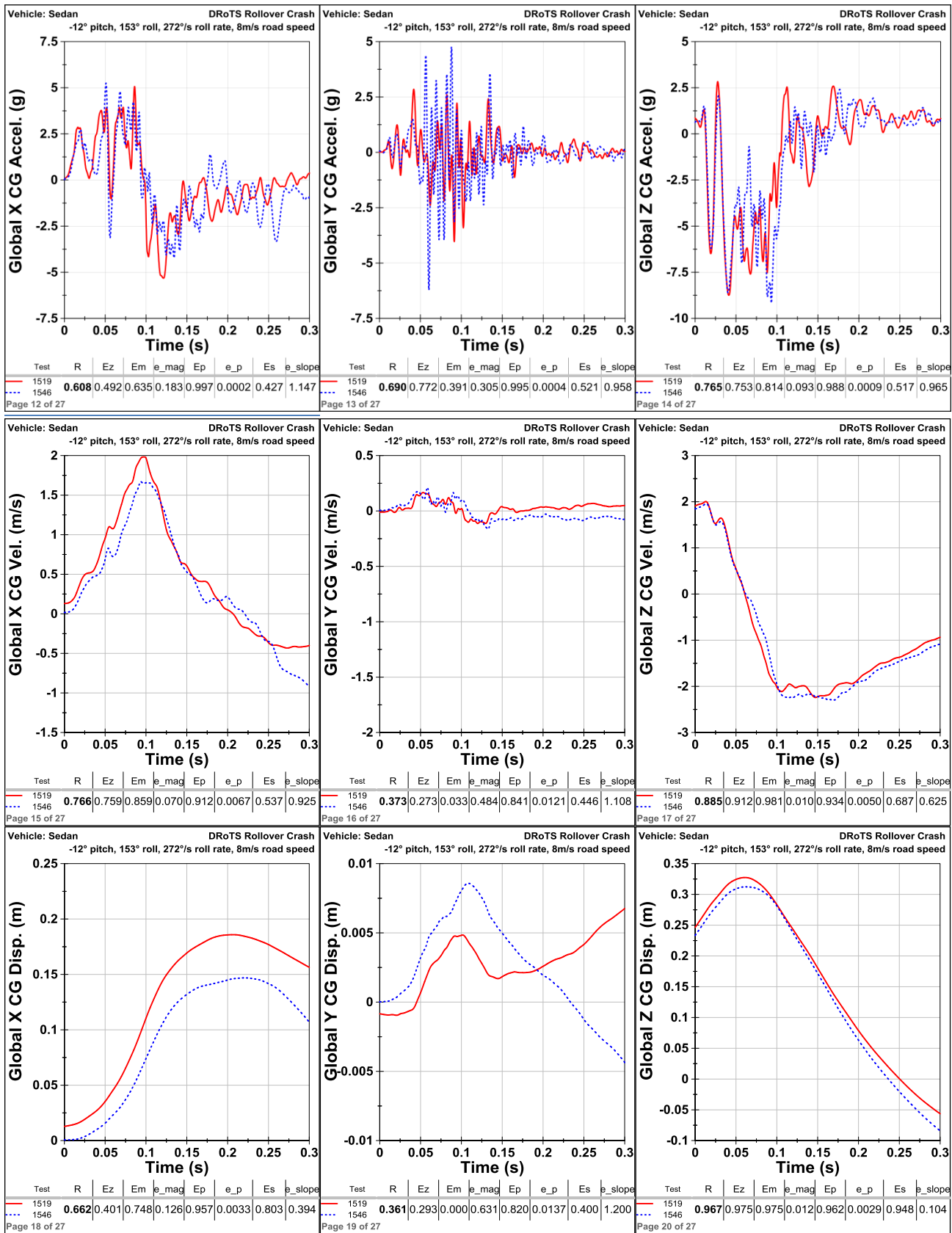


Figure A 2: Global X', Y', and Z' CG acceleration, velocity and displacement time histories, Tests 1519 vs. 1546

APPENDIX B

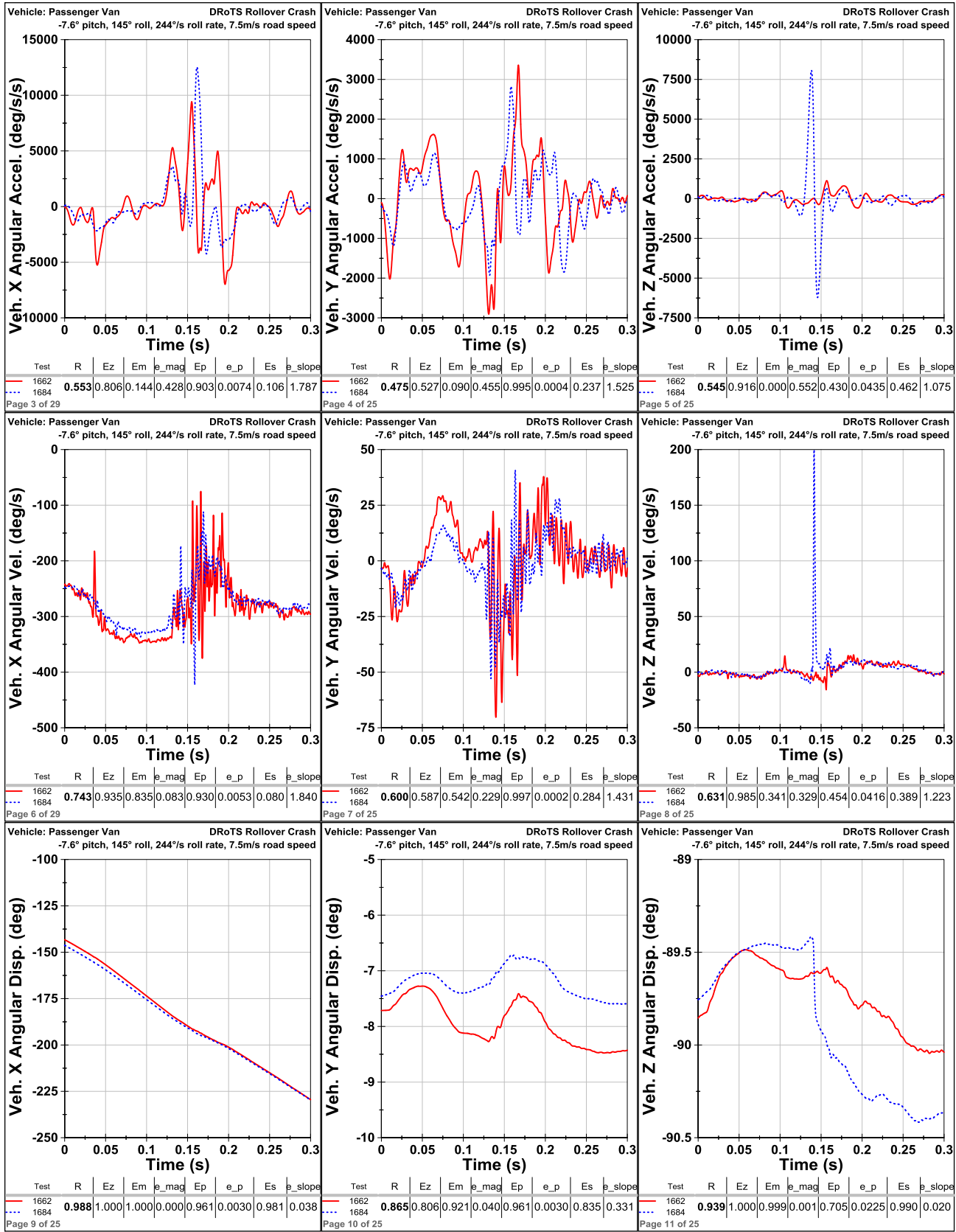


Figure B 1: Vehicle local X, Y, and Z angular acceleration, angular velocity, angular displacement time histories, Tests 1662 vs. 1684

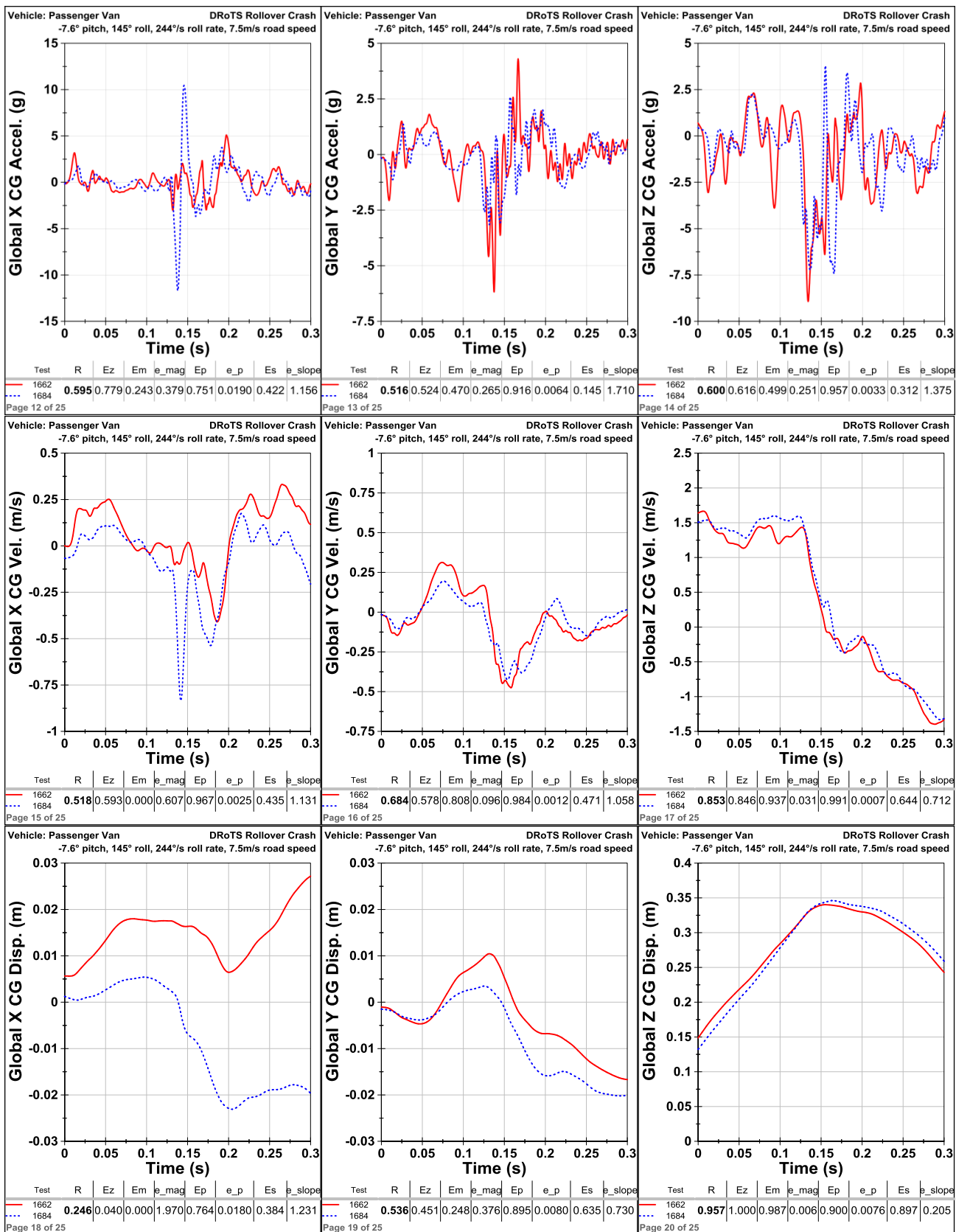


Figure B 2: Global X', Y', and Z' CG acceleration, velocity and displacement time histories, Tests 1662 vs. 1684

APPENDIX C

Signal Analysis of SOI and Oblique Moving Deformable Barrier Tests

C.Cruze 7431vs7852 Oblique	Unit	Ez	Ep	e_p	Em	e_mag	Es	e_slope	R
VEHICLE CG X	gn	0.870	0.971	0.0011	0.901	0.050	0.475	1.051	0.817
VEHICLE CG Y	gn	0.769	0.859	0.0053	0.535	0.233	0.245	1.511	0.635
VEHICLE CG Z	gn	0.812	0.968	0.0012	0.679	0.161	0.451	1.097	0.745
FLOORPAN - RIGHT FRONT	mm	0.186	0.365	0.0238	0.498	0.251	0.000	2.707	0.247
C.Cruze 7431vs7851 Oblique	Unit	Ez	Ep	e_p	Em	e_mag	Es	e_slope	R
VEHICLE CG X	gn	0.898	1.000	0.0000	0.898	0.051	0.514	0.972	0.842
VEHICLE CG Y	gn	0.744	0.984	0.0006	0.468	0.266	0.393	1.213	0.667
VEHICLE CG Z	gn	0.778	0.947	0.0020	0.583	0.208	0.505	0.990	0.718
FLOORPAN - RIGHT FRONT	mm	0.037	0.403	0.0224	0.000	0.658	0.000	7.035	0.095
C.Cruze 7852vs7851 Oblique	Unit	Ez	Ep	e_p	Em	e_mag	Es	e_slope	R
VEHICLE CG X	gn	0.935	0.989	0.0004	0.899	0.050	0.533	0.935	0.858
VEHICLE CG Y	gn	0.765	0.643	0.0134	0.000	0.794	0.444	1.112	0.523
VEHICLE CG Z	gn	0.753	0.968	0.0012	0.583	0.209	0.270	1.461	0.666
FLOORPAN - RIGHT FRONT	mm	0.185	0.813	0.007	0.000	0.582	0.556	0.888	0.348
C.Cruze 7432vs.7773 SOI	Unit	Ez	Ep	e_p	Em	e_mag	Es	e_slope	R
VEHICLE CG X	gn	0.834	0.976	0.0009	0.844	0.078	0.300	1.400	0.758
VEHICLE CG Y	gn	0.450	0.768	0.0087	0.344	0.328	0.190	1.620	0.441
VEHICLE CG Z	gn	0.665	0.965	0.0013	0.423	0.289	0.330	1.340	0.610
FLOORPAN - RIGHT FRONT	mm	0.019	0.032	0.0363	0.000	167.411	0.000	6.461	0.014
C.Cruze 7432vs.7867 SOI	Unit	Ez	Ep	e_p	Em	e_mag	Es	e_slope	R
VEHICLE CG X	gn	0.888	0.992	0.0003	0.879	0.061	0.339	1.321	0.797
VEHICLE CG Y	gn	0.561	0.936	0.0024	0.529	0.236	0.253	1.493	0.568
VEHICLE CG Z	gn	0.383	0.539	0.0173	0.165	0.418	0.371	1.258	0.368
FLOORPAN - RIGHT FRONT	mm	0.250	0.717	0.0106	0.000	1.046	0.241	1.518	0.292
C.Cruze 7773vs.7867 SOI	Unit	Ez	Ep	e_p	Em	e_mag	Es	e_slope	R
VEHICLE CG X	gn	0.972	1.000	0	0.935	0.033	0.680	0.641	0.912
VEHICLE CG Y	gn	0.641	0.989	0.0004	0.183	0.409	0.339	1.323	0.559
VEHICLE CG Z	gn	0.465	0.677	0.0121	0.091	0.454	0.360	1.279	0.412
FLOORPAN - RIGHT FRONT	mm	0.035	0.000	0.0377	0.000	54.089	0.000	5.237	0.014

APPENDIX D

Signal Analysis IIHS small overlap frontal crash tests

2009 Mit. Galant	Unit	Ez	Ep	e_p	Em	e_mag	Es	e_slope	R
Vehicle X Accel.	gn	0.826	0.973	0.0014	0.904	0.048	0.375	1.250	0.781
Vehicle Y Accel.	gn	0.801	0.992	0.0004	0.775	0.112	0.466	1.068	0.767
Vehicle Z Accel.	gn	0.577	0.976	0.0012	0.545	0.228	0.442	1.117	0.624
Vehicle Resultant Accel.	gn	0.845	0.976	0.0012	0.942	0.029	0.310	1.380	0.784

2012 Acura TL	Unit	Ez	Ep	e_p	Em	e_mag	Es	e_slope	R
Vehicle X Accel.	gn	0.821	0.976	0.0012	0.796	0.102	0.437	1.125	0.770
Vehicle Y Accel.	gn	0.688	0.990	0.0005	0.763	0.118	0.464	1.071	0.719
Vehicle Z Accel.	gn	0.749	0.978	0.0011	0.703	0.148	0.377	1.246	0.711
Vehicle Resultant Accel.	gn	0.890	0.986	0.0007	0.893	0.054	0.432	1.137	0.818

2012 Acura TSX	Unit	Ez	Ep	e_p	Em	e_mag	Es	e_slope	R
Vehicle X Accel.	gn	0.774	0.971	0.0015	0.820	0.090	0.361	1.277	0.740
Vehicle Y Accel.	gn	0.814	0.841	0.0081	0.700	0.150	0.462	1.077	0.726
Vehicle Z Accel.	gn	0.755	0.980	0.001	0.720	0.140	0.456	1.087	0.733
Vehicle Resultant Accel.	gn	0.833	0.988	0.0006	0.878	0.061	0.468	1.064	0.800

2012 Volvo S60	Unit	Ez	Ep	e_p	Em	e_mag	Es	e_slope	R
Vehicle X Accel.	gn	0.547	0.443	0.0284	0.746	0.127	0.020	1.961	0.460
Vehicle Y Accel.	gn	0.535	0.600	0.0204	0.609	0.196	0.068	1.863	0.469
Vehicle Z Accel.	gn	0.223	0.009	0.0505	0.000	0.826	0.121	1.758	0.115
Vehicle Resultant Accel.	gn	0.392	0.315	0.0349	0.376	0.312	0.144	1.711	0.324

2008 Ford Fusion 02vs04	Unit	Ez	Ep	e_p	Em	e_mag	Es	e_slope	R
Vehicle X Accel.	gn	0.820	0.988	0.0006	0.775	0.113	0.512	0.976	0.783
Vehicle Y Accel.	gn	0.735	1.000	0	0.801	0.100	0.486	1.027	0.752
Vehicle Z Accel.	gn	0.744	0.979	0.0011	0.000	0.725	0.412	1.176	0.576
Vehicle Resultant Accel.	gn	0.855	0.982	0.0009	0.865	0.067	0.415	1.170	0.794

2008 Ford Fusion 02vs12	Unit	Ez	Ep	e_p	Em	e_mag	Es	e_slope	R
Vehicle X Accel.	gn	0.819	0.996	0.0002	0.832	0.084	0.460	1.080	0.785
Vehicle Y Accel.	gn	0.733	0.994	0.0003	0.766	0.117	0.500	1.001	0.745
Vehicle Z Accel.	gn	0.846	0.984	0.0008	0.603	0.199	0.463	1.074	0.748
Vehicle Resultant Accel.	gn	0.899	0.979	0.0011	0.843	0.079	0.236	1.528	0.771

2008 Ford Fusion 04vs12	Unit	Ez	Ep	e_p	Em	e_mag	Es	e_slope	R
Vehicle X Accel.	gn	0.769	0.969	0.0016	0.747	0.126	0.369	1.261	0.725
Vehicle Y Accel.	gn	0.713	0.988	0.0006	0.813	0.093	0.421	1.159	0.729
Vehicle Z Accel.	gn	0.702	0.961	0.002	0.438	0.281	0.305	1.390	0.621
Vehicle Resultant Accel.	gn	0.822	0.957	0.0022	0.800	0.100	0.295	1.410	0.739

APPENDIX E

Signal Analysis of Frontal Offset Crash Tests

Saab900	Unit	Ez	Ep	e_p	Em	e_mag	Es	e_slope	R
VehXAcc	gn	0.874	0.995	0.0003	0.916	0.042	0.466	1.068	0.825
VehYAcc	gn	0.773	0.965	0.0022	0.673	0.164	0.253	1.494	0.688
VehZAcc	gn	0.859	0.892	0.0069	0.729	0.136	0.318	1.363	0.732
VehResultantAcc	gn	0.939	0.991	0.0006	0.926	0.037	0.526	0.949	0.864

Dodge Neon	Unit	Ez	Ep	e_p	Em	e_mag	Es	e_slope	R
VehXAcc	gn	0.893	0.975	0.0016	0.870	0.065	0.306	1.388	0.787
VehYAcc	gn	0.914	0.981	0.0012	0.803	0.098	0.432	1.136	0.809
VehZAcc	gn	0.791	0.969	0.002	0.510	0.245	0.336	1.327	0.679
VehResultantAcc	gn	0.885	0.962	0.0024	0.909	0.046	0.285	1.430	0.785

Hyundai Elantra	Unit	Ez	Ep	e_p	Em	e_mag	Es	e_slope	R
VehXAcc	gn	0.840	0.904	0.0061	0.871	0.065	0.348	1.305	0.760
VehYAcc	gn	0.878	0.991	0.0006	0.840	0.080	0.503	0.995	0.818
VehZAcc	gn	0.629	0.890	0.007	0.553	0.224	0.334	1.332	0.607
VehResultantAcc	gn	0.847	0.931	0.0044	0.874	0.063	0.382	1.235	0.776

Infinity Q45	Unit	Ez	Ep	e_p	Em	e_mag	Es	e_slope	R
VehXAcc	gn	0.896	0.997	0.0002	0.887	0.057	0.484	1.033	0.832
VehYAcc	gn	0.730	0.987	0.0008	0.572	0.214	0.447	1.106	0.693
VehZAcc	gn	0.647	0.978	0.0014	0.327	0.336	0.472	1.057	0.614
VehResultantAcc	gn	0.870	0.989	0.0007	0.772	0.114	0.516	0.968	0.803

Pontiac Trans Sport	Unit	Ez	Ep	e_p	Em	e_mag	Es	e_slope	R
VehXAcc	gn	0.911	1.000	0	0.924	0.038	0.357	1.287	0.820
VehYAcc	gn	0.741	0.981	0.0012	0.586	0.207	0.259	1.481	0.662
VehZAcc	gn	0.566	0.992	0.0005	0.000	1.301	0.000	2.950	0.425
VehResultantAcc	gn	0.896	0.987	0.0008	0.942	0.029	0.333	1.333	0.811

APPENDIX F

Signal Analysis of Frontal Crash Test

2010 Mazda 3	Unit	Ez	Ep	e_p	Em	e_mag	Es	e_slope	R	Grade
Seat-Left Rear X	gn	0.842	0.977	0.001	0.941	0.030	0.543	0.914	0.829	Good
Seat-Right Rear X	gn	0.867	1.000	0.000	0.934	0.033	0.458	1.085	0.825	Good
Engine	gn	0.933	0.992	0.000	0.889	0.056	0.700	0.599	0.890	Good
Brake Caliper-Right	gn	0.810	0.920	0.003	0.754	0.123	0.465	1.070	0.752	Fair
Seat-Left Rear Z	gn	0.439	0.876	0.005	0.000	1.059	0.050	1.900	0.361	Poor
Seat-Right Rear Z	gn	0.500	0.977	0.001	0.224	0.388	0.210	1.581	0.482	Poor
Sum Total Force	N	0.844	0.899	0.004	0.961	0.020	0.562	0.877	0.822	Good

2010 Lexus RX350	Unit	Ez	Ep	e_p	Em	e_mag	Es	e_slope	R	Grade
FloorPan-Left Rear X	gn	0.928	0.946	0.002	0.963	0.018	0.642	0.717	0.881	Good
FloorPan-Right Rear X	gn	0.905	0.941	0.002	0.948	0.026	0.661	0.679	0.872	Good
Engine	gn	0.949	0.972	0.001	0.737	0.131	0.792	0.417	0.880	Good
Engine	gn	0.920	0.979	0.001	0.833	0.083	0.663	0.675	0.863	Good
Brake Caliper-Right	gn	0.827	0.951	0.002	0.388	0.306	0.438	1.123	0.686	Fair
FloorPan-Left Rear Z	gn	0.438	0.985	0.001	0.000	0.640	0.255	1.489	0.423	Poor
FloorPan-Right Rear Z	gn	0.498	0.946	0.002	0.000	0.711	0.204	1.591	0.429	Poor
Sum Total Force	N	0.871	0.920	0.003	0.945	0.027	0.802	0.396	0.882	Good

2010 Kia Soul	Unit	Ez	Ep	e_p	Em	e_mag	Es	e_slope	R	Grade
Seat-Left Rear X	gn	0.818	0.964	0.001	0.803	0.099	0.329	1.342	0.746	Fair
Seat-Right Rear X	gn	0.878	0.959	0.002	0.917	0.042	0.686	0.628	0.863	Good
Engine	gn	0.933	0.995	0.000	0.789	0.106	0.626	0.749	0.855	Good
Engine	gn	0.883	0.990	0.000	0.514	0.243	0.619	0.762	0.778	Fair
Brake Caliper-Left	gn	0.776	0.822	0.007	0.665	0.168	0.495	1.010	0.707	Fair
Brake Caliper-Right	gn	0.819	0.889	0.004	0.612	0.194	0.545	0.911	0.737	Fair
Seat-Left Rear Z	gn	0.566	0.969	0.001	0.151	0.425	0.230	1.539	0.497	Poor
Seat-Right Rear Z	gn	0.559	0.615	0.015	0.432	0.284	0.364	1.272	0.506	Poor
Sum Total Force	N	0.908	0.954	0.002	0.972	0.014	0.655	0.690	0.879	Good

2010 Hyundai Genesis	Unit	Ez	Ep	e_p	Em	e_mag	Es	e_slope	R	Grade
Seat-Left Rear X	gn	0.837	0.956	0.002	0.718	0.141	0.458	1.083	0.761	Fair
Seat-Right Rear X	gn	0.852	0.972	0.001	0.837	0.082	0.497	1.006	0.802	Good
Engine	gn	0.948	0.995	0.000	0.809	0.095	0.614	0.772	0.863	Good
Brake Caliper-Left	gn	0.000	0.621	0.015	0.000	76.209	0.000	5.048	0.124	Poor
Brake Caliper-Right	gn	0.841	0.964	0.001	0.773	0.114	0.566	0.867	0.797	Fair
Seat-Left Rear Z	gn	0.770	0.987	0.001	0.320	0.340	0.491	1.018	0.668	Fair
Seat-Right Rear Z	gn	0.673	0.946	0.002	0.620	0.190	0.351	1.299	0.653	Fair

Sum Total Force	N	0.986	0.987	0.001	0.984	0.008	0.796	0.408	0.948	Excellent
2010 Honda Insight	Unit	Ez	Ep	e_p	Em	e_mag	Es	e_slope	R	Grade
FloorPan-Left Rear X	gn	0.830	0.938	0.002	0.875	0.063	0.354	1.291	0.765	Fair
FloorPan-Right Rear X	gn	0.842	0.987	0.001	0.846	0.077	0.445	1.109	0.792	Fair
Engine	gn	0.695	0.985	0.001	0.319	0.341	0.505	0.990	0.640	Fair
Engine	gn	0.862	0.964	0.001	0.692	0.154	0.461	1.078	0.768	Fair
Brake Caliper-Left	gn	0.736	0.739	0.010	0.000	0.851	0.000	2.013	0.442	Poor
Brake Caliper-Right	gn	0.796	0.881	0.005	0.676	0.162	0.399	1.202	0.710	Fair
FloorPan-Left Rear Z	gn	0.817	0.948	0.002	0.430	0.285	0.548	0.903	0.712	Fair
FloorPan-Right Rear Z	gn	0.704	0.982	0.001	0.609	0.195	0.611	0.777	0.722	Fair
Sum Total Force	N	0.915	0.977	0.001	0.944	0.028	0.680	0.641	0.886	Good

2008 Cadillac CTS	Unit	Ez	Ep	e_p	Em	e_mag	Es	e_slope	R	Grade
Sill-Left Rear X	gn	0.889	0.990	0.000	0.707	0.147	0.487	1.027	0.792	Fair
Sil-Right Rear X	gn	0.925	1.000	0.000	0.939	0.031	0.689	0.623	0.895	Good
Brake Caliper-Left	gn	0.715	0.814	0.007	0.000	0.693	0.284	1.432	0.506	Poor
Brake Caliper-Right	gn	0.799	0.987	0.001	0.795	0.103	0.404	1.191	0.757	Fair
Sill-Left Rear Z	gn	0.551	0.982	0.001	0.675	0.162	0.370	1.260	0.626	Fair
Sil-Right Rear Z	gn	0.564	0.985	0.001	0.485	0.258	0.439	1.123	0.607	Fair
Sum Total Force	N	0.944	0.977	0.001	0.924	0.038	0.812	0.375	0.920	Good

2005 Toyota Corolla	Unit	Ez	Ep	e_p	Em	e_mag	Es	e_slope	R	Grade
Seat-Left Rear X	gn	0.844	0.987	0.001	0.905	0.047	0.507	0.986	0.818	Good
Seat-Right Rear X	gn	0.502	0.979	0.001	0.113	0.444	0.298	1.404	0.479	Poor
Engine	gn	0.844	0.995	0.000	0.909	0.045	0.601	0.798	0.839	Good
Engine	gn	0.510	0.982	0.001	0.000	0.604	0.146	1.708	0.430	Poor
Brake Caliper-Left	gn	0.330	0.058	0.037	0.000	0.989	0.466	1.068	0.237	Poor
Brake Caliper-Right	gn	0.949	0.987	0.001	0.882	0.059	0.752	0.496	0.904	Good
Seat-Left Rear Z	gn	0.835	0.974	0.001	0.740	0.130	0.341	1.318	0.745	Fair
Seat-Right Rear Z	gn	0.818	0.982	0.001	0.784	0.108	0.485	1.029	0.777	Fair
Sum Total Force	N	0.904	0.956	0.002	0.973	0.013	0.680	0.640	0.883	Good

2005 Honda Odyssey	Unit	Ez	Ep	e_p	Em	e_mag	Es	e_slope	R	Grade
Seat-Left Rear	gn	0.862	0.992	0.000	0.452	0.274	0.502	0.996	0.734	Fair
Seat-Right Rear	gn	0.857	0.997	0.000	0.899	0.050	0.536	0.928	0.829	Good
Engine	gn	0.985	1.000	0.000	0.821	0.089	0.745	0.509	0.907	Good
Brake Caliper-Left	gn	0.311	0.000	0.046	0.000	1.005	0.407	1.187	0.206	Poor
Brake Caliper-Right	gn	0.676	0.935	0.003	0.000	0.503	0.290	1.420	0.516	Poor
Dashpanel-Center	gn	0.773	0.943	0.002	0.866	0.067	0.240	1.519	0.719	Fair
Sum Total Force	N	0.903	0.977	0.001	0.972	0.014	0.695	0.610	0.890	Good

2003 Chevrolet Silverado	Unit	Ez	Ep	e_p	Em	e_mag	Es	e_slope	R	Grade
Seat-Left Rear	gn	0.830	0.974	0.001	0.897	0.052	0.545	0.910	0.815	Good
Seat-Right Rear	gn	0.814	0.979	0.001	0.839	0.080	0.433	1.134	0.776	Fair
Engine	gn	0.837	0.920	0.003	0.659	0.170	0.339	1.322	0.719	Fair
Brake Caliper-Left	gn	0.861	0.966	0.001	0.455	0.272	0.455	1.091	0.720	Fair
Brake Caliper-Right	gn	0.734	0.979	0.001	0.705	0.147	0.491	1.018	0.729	Fair
Sum Total Force	N	0.889	0.966	0.001	0.956	0.022	0.550	0.899	0.850	Good

2002 Toyota Tundra	Unit	Ez	Ep	e_p	Em	e_mag	Es	e_slope	R	Grade
Seat-Left Rear	gn	0.909	0.997	0.000	0.935	0.032	0.574	0.853	0.865	Good
Seat-Right Rear	gn	0.891	0.997	0.000	0.914	0.043	0.596	0.808	0.858	Good
Engine	gn	0.980	1.000	0.000	0.920	0.040	0.805	0.390	0.937	Good
Engine	gn	0.944	0.995	0.000	0.548	0.226	0.620	0.760	0.810	Good
Brake Caliper-Right	gn	0.672	0.000	0.045	0.000	0.812	0.466	1.067	0.362	Poor
Brake Caliper-left	gn	0.629	0.935	0.003	0.000	1.052	0.000	2.376	0.439	Poor
Dashpanel-Center	gn	0.702	0.943	0.002	0.529	0.235	0.447	1.106	0.665	Fair
Sum Total Force	N	0.942	0.961	0.002	0.973	0.014	0.545	0.910	0.872	Good

2002 Dodge Ram	Unit	Ez	Ep	e_p	Em	e_mag	Es	e_slope	R	Grade
Seat-Left Rear	gn	0.803	0.941	0.002	0.911	0.045	0.196	1.608	0.731	Fair
Seat-Right Rear	gn	0.824	0.951	0.002	0.917	0.042	0.322	1.356	0.768	Fair
Brake Caliper-Right	gn	0.539	0.316	0.026	0.092	0.454	0.070	1.861	0.311	Poor
Dashpanel-Center	gn	0.700	0.990	0.000	0.674	0.163	0.380	1.241	0.689	Fair
Brake Caliper-left	gn	0.608	0.270	0.028	0.000	0.606	0.179	1.641	0.333	Poor
Sum Total Force	N	0.893	0.985	0.001	0.929	0.035	0.524	0.952	0.845	Good

2002 Chevrolet Trailblazer	Unit	Ez	Ep	e_p	Em	e_mag	Es	e_slope	R	Grade
Seat-Left Rear	gn	0.938	0.985	0.001	0.929	0.035	0.581	0.837	0.874	Good
Seat-Right Rear	gn	0.931	0.987	0.001	0.933	0.034	0.526	0.947	0.862	Good
Engine	gn	0.914	0.951	0.002	0.842	0.079	0.515	0.970	0.827	Good
Dashpanel-Center	gn	0.734	0.943	0.002	0.572	0.214	0.448	1.103	0.686	Fair
Sum Total Force	N	0.965	0.974	0.001	0.963	0.019	0.588	0.823	0.891	Good

APPENDIX G

Signal Analysis of DRoTS Tests

1546vs1519	Unit	Ez	Ep	e_p	Em	e_mag	Es	e_slope	R	Grade
Veh. X Angular Accel.	°/s/s	0.603	0.959	0.003	0.094	0.453	0.249	1.503	0.502	poor
Veh. Y Angular Accel.	°/s/s	0.508	0.849	0.012	0.563	0.219	0.482	1.035	0.582	fair
Veh. Z Angular Accel.	°/s/s	0.495	0.895	0.008	0.627	0.187	0.310	1.381	0.564	poor
Veh. X Angular Vel.	°/s	0.711	0.373	0.048	0.826	0.087	0.406	1.189	0.606	fair
Veh. Y Angular Vel.	°/s	0.713	0.916	0.006	0.444	0.278	0.563	0.874	0.670	fair
Veh. Z Angular Vel.	°/s	0.655	0.854	0.011	0.819	0.090	0.262	1.477	0.649	fair
Veh. X Angular Disp.	°	1.000	0.193	0.062	0.981	0.010	0.940	0.120	0.823	good
Veh. Y Angular Disp.	°	0.857	0.877	0.009	0.944	0.028	0.842	0.316	0.875	good
Veh. Z Angular Disp.	°	1.000	0.788	0.016	0.999	0.001	0.980	0.040	0.953	excellent
Global X CG Accel.	gn	0.492	0.997	0.000	0.635	0.183	0.427	1.147	0.608	fair
Global Y CG Accel.	gn	0.772	0.995	0.000	0.391	0.305	0.521	0.958	0.690	fair
Global Z CG Accel.	gn	0.753	0.988	0.001	0.814	0.093	0.517	0.965	0.765	fair
Global X CG Vel.	m/s	0.759	0.912	0.007	0.859	0.070	0.537	0.925	0.766	fair
Global Y CG Vel.	m/s	0.273	0.841	0.012	0.033	0.484	0.446	1.108	0.373	poor
Global Z CG Vel.	m/s	0.912	0.934	0.005	0.981	0.010	0.687	0.625	0.885	good
Global X CG Disp.	mm	0.401	0.957	0.003	0.748	0.126	0.803	0.394	0.662	fair
Global Y CG Disp.	mm	0.293	0.820	0.014	0.000	0.631	0.400	1.200	0.361	poor
Global Z CG Disp.	mm	0.975	0.962	0.003	0.975	0.012	0.948	0.104	0.967	excellent
Veh. X CG Accel.	gn	0.788	0.996	0.000	0.480	0.260	0.507	0.986	0.712	fair
Veh. Y CG Accel.	gn	0.730	0.937	0.005	0.875	0.062	0.289	1.422	0.712	fair
Veh. Z CG Accel.	gn	0.624	1.000	0.000	0.611	0.195	0.515	0.969	0.675	fair
Total Vertical Load	N	0.848	0.988	0.001	0.923	0.038	0.604	0.793	0.842	good
Road Velocity	m/s	1.000	0.904	0.007	0.987	0.007	0.550	0.899	0.888	good
A pillar res. Disp.	mm	0.985	0.991	0.001	0.944	0.028	0.866	0.267	0.954	excellent
B pill res. Disp.	mm	0.934	0.980	0.002	0.959	0.021	0.701	0.597	0.902	good
A pillar X Disp.	mm	0.212	0.984	0.001	0.389	0.306	0.514	0.971	0.462	poor
A pillar Y Disp.	mm	0.994	0.999	0.000	0.955	0.023	0.785	0.429	0.945	excellent
A pillar Z Disp.	mm	0.977	0.993	0.001	0.953	0.023	0.745	0.509	0.929	good
A pillar res. Disp.	mm	0.985	0.991	0.001	0.944	0.028	0.866	0.267	0.954	excellent
B pill X Disp.	mm	0.288	0.824	0.013	0.639	0.181	0.143	1.713	0.436	poor
B pill Y Disp.	mm	0.852	0.993	0.001	0.957	0.021	0.466	1.067	0.824	good
B pill Z Disp.	mm	0.954	0.982	0.001	0.990	0.005	0.402	1.197	0.856	good
B pill res. Disp.	mm	0.934	0.980	0.002	0.959	0.021	0.701	0.597	0.902	good
Eq. Res. Acc (Global X & Z)	gn	0.787	0.988	0.001	0.872	0.064	0.468	1.064	0.780	fair

1662vs1684	Unit	Ez	Ep	e_p	Em	e_mag	Es	e_slope	R	Grade
Veh. X Angular Accel.	°/s/s	0.806	0.903	0.007	0.144	0.428	0.106	1.787	0.553	poor
Veh. Y Angular Accel.	°/s/s	0.527	0.995	0.000	0.090	0.455	0.237	1.525	0.475	poor
Veh. Z Angular Accel.	°/s/s	0.916	0.430	0.044	0.000	0.552	0.462	1.075	0.545	poor
Veh. X Angular Vel.	°/s	0.935	0.930	0.005	0.835	0.083	0.080	1.840	0.743	fair
Veh. Y Angular Vel.	°/s	0.587	0.997	0.000	0.542	0.229	0.284	1.431	0.600	fair
Veh. Z Angular Vel.	°/s	0.985	0.454	0.042	0.341	0.329	0.389	1.223	0.631	fair
Veh. X Angular Disp.	°	1.000	0.961	0.003	1.000	0.000	0.981	0.038	0.988	excellent
Veh. Y Angular Disp.	°	0.806	0.961	0.003	0.921	0.040	0.835	0.331	0.865	good
Veh. Z Angular Disp.	°	1.000	0.705	0.022	0.999	0.001	0.990	0.020	0.939	good
Global X CG Accel.	gn	0.779	0.751	0.019	0.243	0.379	0.422	1.156	0.595	fair
Global Y CG Accel.	gn	0.524	0.916	0.006	0.470	0.265	0.145	1.710	0.516	poor
Global Z CG Accel.	gn	0.616	0.957	0.003	0.499	0.251	0.312	1.375	0.600	fair
Global X CG Vel.	m/s	0.593	0.967	0.003	0.000	0.607	0.435	1.131	0.518	poor
Global Y CG Vel.	m/s	0.578	0.984	0.001	0.808	0.096	0.471	1.058	0.684	fair
Global Z CG Vel.	m/s	0.846	0.991	0.001	0.937	0.031	0.644	0.712	0.853	good
Global X CG Disp.	m	0.040	0.764	0.018	0.000	1.970	0.384	1.231	0.246	poor
Global Y CG Disp.	m	0.451	0.895	0.008	0.248	0.376	0.635	0.730	0.536	poor
Global Z CG Disp.	m	1.000	0.900	0.008	0.987	0.006	0.897	0.205	0.957	excellent
Veh. X CG Accel.	gn	0.516	0.915	0.007	0.503	0.248	0.167	1.665	0.524	poor
Veh. Y CG Accel.	gn	0.844	0.958	0.003	0.025	0.487	0.395	1.209	0.613	fair
Veh. Z CG Accel.	gn	0.616	0.951	0.004	0.340	0.330	0.282	1.436	0.561	poor
Total Vertical Load	N	0.902	0.977	0.001	0.848	0.076	0.474	1.052	0.821	good
Road Velocity	m/s	0.986	0.854	0.011	0.993	0.004	0.888	0.223	0.941	excellent
Eq. Res. Acc (Global X & Z)	gn	0.796	0.949	0.004	0.647	0.176	0.309	1.382	0.699	fair

APPENDIX H

Signal Analysis of DRS Tests DRS Testing

Ford Explorer V1 vs V2	Unit	Ez	Ep	e_p	Em	e_mag	Es	e_slope	R	Grade
Veh. X Angular Accel.	°/s/s	0.968	0.964	0.018	0	0.770	0.382	1.236	0.657	Fair
Veh. Y Angular Accel.	°/s/s	0.970	0.988	0.006	0	1.354	0.219	1.562	0.630	Fair
Veh. Z Angular Accel.	°/s/s	0.961	0.791	0.1049	0	2.065	0	2.632	0.543	Poor
Veh. X Angular Vel.	°/s	0.929	0.994	0.0028	0.889	0.055	0.106	1.788	0.769	Fair
Veh. Y Angular Vel.	°/s	0.809	0.979	0.0103	0	0.502	0.087	1.826	0.537	Poor
Veh. Z Angular Vel.	°/s	0.941	0.964	0.0179	0.284	0.358	0.317	1.367	0.690	Fair
Veh. X Angular Disp.	°	1.	0.997	0.0016	0.982	0.009	0.949	0.102	0.986	Excellent
Veh. Y Angular Disp.	°	0.565	0.918	0.0409	0.398	0.301	0.348	1.303	0.559	Poor
Veh. Z Angular Disp.	°	0.783	0	0.6015	0.006	0.497	0.328	1.344	0.380	Poor
Global X CG Accel.	gn	0.964	0.997	0.0015	0	0.815	0.309	1.383	0.647	Fair
Global Y CG Accel.	gn	0.972	0.984	0.0081	0	0.785	0.328	1.344	0.651	Fair
Global Z CG Accel.	gn	0.962	0.985	0.0075	0	0.657	0.262	1.477	0.634	Fair
Global X CG Vel.	m/s	0.197	0.831	0.0849	0.025	0.488	0.202	1.595	0.291	Por
Global Y CG Vel.	m/s	1	0.991	0.0047	0.993	0.003	0.694	0.611	0.936	Good
Global Z CG Vel.	m/s	0.916	0.997	0.0017	0.859	0.070	0.528	0.944	0.843	Good
Global X CG Disp.	m	0.199	0	0.6015	0	1.980	0.000	2.895	0.080	Poor
Global Y CG Disp.	m	1.	0.986	0.0068	0.995	0.002	0.982	0.035	0.993	Excellent
Global Z CG Disp.	m	0.777	0.981	0.0094	0.877	0.062	0.901	0.198	0.862	Good
Ford Explorer V1 vs V3	Unit	Ez	Ep	e_p	Em	e_mag	Es	e_slope	R	Grade
Veh. X Angular Accel.	°/s/s	0.966	0.949	0.0258	0	1.001	0.194	1.611	0.615	Fair
Veh. Y Angular Accel.	°/s/s	0.958	0.888	0.056	0	0.902	0.381	1.238	0.637	Fair
Veh. Z Angular Accel.	°/s/s	0.970	0.893	0.0536	0	0.962	0.262	1.476	0.619	Fair
Veh. X Angular Vel.	°/s	0.557	0.584	0.2084	0.529	0.235	0.219	1.562	0.489	Poor
Veh. Y Angular Vel.	°/s	0.729	0.990	0.0048	0.550	0.225	0.277	1.447	0.655	Fair
Veh. Z Angular Vel.	°/s	0.645	0.401	0.3004	0.520	0.240	0.000	2.071	0.442	Poor
Veh. X Angular Disp.	°	0.715	0.010	0.496	0.792	0.104	0.480	1.039	0.543	Poor
Veh. Y Angular Disp.	°	0.306	0.000	0.6015	0.000	4.035	0.000	2.127	0.122	Por
Veh. Z Angular Disp.	°	0.648	0.000	0.6015	0.378	0.311	0.245	1.509	0.384	Poor
Global X CG Accel.	gn	0.948	0.928	0.0359	0	0.864	0.266	1.467	0.618	Fair
Global Y CG Accel.	gn	0.956	0.897	0.0517	0	0.811	0.324	1.352	0.626	Fair
Global Z CG Accel.	gn	0.965	0.937	0.0315	0	0.702	0.270	1.460	0.627	Fair
Global X CG Vel.	m/s	0.178	0.327	0.3371	0.245	0.377	0.194	1.612	0.225	Poor
Global Y CG Vel.	m/s	0.914	0.966	0.0171	0.951	0.024	0.665	0.669	0.882	Good
Global Z CG Vel.	m/s	0.686	0.929	0.0358	0.712	0.144	0.514	0.973	0.705	Fair
Global X CG Disp.	m	0.207	0.000	0.6015	0	1.515	0.047	1.906	0.092	Poor

Global Y CG Disp.	m	0.851	0.811	0.0947	0.941	0.030	0.832	0.336	0.857	Good
Global Z CG Disp.	m	0.775	1	0	0.831	0.085	0.785	0.429	0.833	Good
Ford Explorer V2 vs V3	Unit	Ez	Ep	e_p	Em	e_mag	Es	e_slope	R	Grade
Veh. X Angular Accel.	°/s/s	0.965	0.722	0.1393	0	0.818	0.308	1.384	0.592	Fair
Veh. Y Angular Accel.	°/s/s	0.944	0.720	0.1403	0	2.013	0	2.673	0.522	Poor
Veh. Z Angular Accel.	°/s/s	0.944	0.893	0.0538	0	2.844	0	3.088	0.556	Poor
Veh. X Angular Vel.	°/s	0.514	0.555	0.223	0.576	0.212	0	2.267	0.432	Poor
Veh. Y Angular Vel.	°/s	0.601	0.937	0.0317	0	1.212	0	2.284	0.428	Poor
Veh. Z Angular Vel.	°/s	0.871	0.761	0.1196	0.282	0.359	0.360	1.280	0.629	Fair
Veh. X Angular Disp.	°	0.637	0.045	0.4788	0.456	0.272	0.526	0.948	0.460	Poor
Veh. Y Angular Disp.	°	0.289	0	0.6015	0	0.930	0	2.202	0.116	Poor
Veh. Z Angular Disp.	°	0.617	0	0.6015	0.368	0.316	0.161	1.679	0.353	poor
Global X CG Accel.	gn	0.956	0.940	0.0301	0	1.122	0.212	1.577	0.613	fair
Global Y CG Accel.	gn	0.957	0.873	0.0635	0	1.206	0.122	1.757	0.582	Fair
Global Z CG Accel.	gn	0.948	0.933	0.0336	0	1.068	0.091	1.819	0.584	Fair
Global X CG Vel.	m/s	0.747	0.882	0.059	0.947	0.026	0.229	1.542	0.711	Fair
Global Y CG Vel.	m/s	0.870	0.976	0.0122	0.949	0.025	0.601	0.799	0.853	Good
Global Z CG Vel.	m/s	0.691	0.922	0.0393	0.593	0.203	0.395	1.211	0.658	Fair
Global X CG Disp.	m	0.817	0.690	0.1552	0.965	0.017	0.592	0.817	0.776	Fair
Global Y CG Disp.	m	0.739	0.801	0.0996	0.895	0.052	0.819	0.363	0.799	Fair
Global Z CG Disp.	m	0.932	0.952	0.0243	0.943	0.028	0.676	0.648	0.887	Good

APPENDIX I

Table I-1: Comparison and variation of overall score with respect to each crash test

	NHTSA Frontal			IIHS Small Overlap			IIHS Frontal Offset		
	<i>Veh. X Acc</i>	<i>Veh. Z Acc</i>	<i>Barrier Force</i>	<i>Veh. X Acc</i>	<i>Veh. Y Acc</i>	<i>Res. Accel</i>	<i>Veh. X Acc</i>	<i>Veh. Y Acc</i>	<i>Res. Accel</i>
N*	12			7			5		
Average R	0.801	0.488	0.885	0.721	0.701	0.719	0.805	0.734	0.808
Min R	0.731	0.315	0.822	0.460	0.469	0.324	0.760	0.662	0.776
Max R	0.881	0.712	0.994	0.785	0.767	0.818	0.832	0.818	0.864
σ/μ (%)	6	27	5	15	14	23	3	9	4
range/μ (%)	19	81	19	45	43	69	9	21	11

	NHTSA SOI				NHTSA Oblique			
	<i>Veh. X Acc</i>	<i>Veh. Y Acc</i>	<i>Res. X & Y Accel</i>	<i>FloorPan-RF Disp</i>	<i>Veh. X Acc</i>	<i>Veh. Y Acc</i>	<i>Res. X & Y Accel</i>	<i>FloorPan-RF Disp</i>
N*	3				3			
Average R	0.822	0.523	0.778	0.107	0.839	0.608	0.794	0.230
Min R	0.758	0.441	0.753	0.014	0.817	0.523	0.759	0.095
Max R	0.912	0.568	0.794	0.292	0.858	0.667	0.820	0.348
σ/μ (%)	8	11	2	123	2	10	3	45
range/μ (%)	19	24	5	260	5	24	8	110

	DRoTS			DRoTS			DRoTS		
	Accel.			Angular			Deformation & Kinetics		
	<i>Global X'</i>	<i>Global Z'</i>	<i>Res. X' & Z'</i>	<i>Vel. X</i>	<i>Vel. Y</i>	<i>Disp X</i>	<i>Road Force</i>	<i>A pillar Disp</i>	<i>B pillar Disp</i>
N*	2			2			2	1	
Average R	0.602	0.683	0.740	0.674	0.635	0.906	0.832	0.954	0.902
Min R	0.595	0.600	0.699	0.606	0.600	0.823	0.821	--	--
Max R	0.608	0.765	0.780	0.743	0.670	0.988	0.842	--	--

	DRS			DRS		
	Accel.			Angular		
	<i>Global X'</i>	<i>Global Z'</i>	<i>Res. X' & Z'</i>	<i>Vel. X</i>	<i>Vel. Y</i>	<i>Disp X</i>
N*	3			3		
Average R	0.620	0.615	0.625	0.563	0.540	0.663
Min R	0.582	0.584	0.592	0.432	0.428	0.460
Max R	0.651	0.634	0.650	0.769	0.655	0.986
σ/μ (%)	5	4	4	26	17	35
range/μ (%)	11	8	9	60	42	79

N*: Number of paired tests

REFERENCES

- Austin, R. (2010). *Roof strength testing and real-world roof intrusion in rollovers*. NHTSA, (DOT HS 811 365) August, 2010.
- Bahling, G., Bundorf, R., & Kaspzyk, G. (1990). Rollover and Drop Tests - The Influence of Roof Strength on Injury Mechanics Using Belted Dummies. *SAE Technical Paper*, 902314. doi:10.4271/902314
- Bahling, G., Bundorf, R., Kaspzyk, G., & Moffatt, E. (1990). Rollover and Drop Tests - The Influence of Roof Strength on Injury Mechanics Using Belted Dummies. *SAE Technical Paper*, 902314. doi:10.4271/902314
- Beard, D. A., & Schlick, T. (2003). Unbiased Rotational Moves for Rigid-Body Dynamics. *Biophysical Journal*, 85, 2973-2976.
- Bish, J., Caplinger, J., D., F., Jordan, A., & Nash, C. (2008). Repeatability of a Dynamic Rollover Test System. *ICRASH International Crashworthiness Conference*. Kyoto, Japan.
- Brumbelow, M. L. (2009, December). Roof Strength and Injury Risk in Rollover Crashes of Passenger Cars and SUVs. *Traffic Injury Prevention*, 584-592. doi:10.1080/15389580903168474
- Carter, J., Habberstad, J., & Croteau, J. (2002). A Comparison of the Controlled Rollover Impact System (CRIS) with the J2114 Rollover Dolly. *SAE Technical Paper*, 2002-01-0694. doi:10.4271/2002-01-0694
- Chirwa, E. C., Stephenson, R. R., Batzer, S. A., & Grzebieta, R. H. (2010). Review of the Jordan Rollover System (JRS) vis-a-vis other dynamic crash test devices. *International Journal of Crashworthiness*, 15(5), 553-569. doi:10.1080/13588265.2010.504373
- Chou, C., McCoy, R., & Le, J. (2005). A Literature Review of Rollover Test Methodologies. *International Journal of Vehicle Safety*, 1(1/2/3), 200-237. doi:10.1504/IJVS.2005.007560
- Chrysler Corporation Petitioner vs. Department of Transportation (United States Court of Appeals, Sixth Circuit December 5, 1972).
- Cooper, E., Moffatt, E., Curzon, A., & Smyth, B. (2001). Repeatable Dynamic Rollover Test Procedure with Controlled Roof Impact. *SAE Technical Paper*, 2001-01-0476. doi:10.4271/2001-01-0476
- Department of Transportation. (2010). *Federal Motor Vehicle Safety Standards: Roof Crush Resistance*. National Highway Traffic Safety Administration.
- DiMasi, F. P. (1995). *Transformation of Nine-Accelerometer-Package (NAP) Data for Replicating Headpart Kinematics and Dynamic Loading*. National Technical Information Service, Department of Commerce. Springfield, VA: NHTSA. Retrieved from <http://www.ntis.gov/search/product.aspx?ABBR=PB96115357>
- Eriksson, L., Hakan, S., Zellmer, H., Fograscher, K., Drexl, B., & Van Slagmaat, M. (2009). Using the Objective Rating Method (ORM) as a Quality Assessment Tool for Physical Tests, Test Methods, and Mathematical Models. *Proceedings of the 21st International Technical Conference on the Enhanced Safety of Vehicles* (pp. 0163-0177). Stuttgart, Germany: (June 15-18, 2009).
- Foltz, P., Kim, T., Kerrigan, J., & Crandall, J. (2011). Vehicle greenhouse shape analysis for design of a parametric test buck for dynamic rollover testing. *Proceedings of the 22nd International Technical Conference on the Enhanced Safety of Vehicles (ESV)* (pp. 0271-0284). Washington, D.C.: (June 13-16, 2011).

- Friedman, D., Jordan, A., Nash, C., Bish, J., Honikman, T., & Sigel, J. (2003). Repeatable Dynamic Rollover Roof Test Fixture. *ASME 2003 International Mechanical Engineering Congress and Exposition*, (pp. 269-270). Washington, D.C. doi:10.1115/IMECE2003-43076
- Friedman, D., Nash, C., & Bish, J. (2007). Observations from Repeatable Dynamic Rollover Tests. *International Journal of Crashworthiness*, 12(1), 67-76. doi:10.1533/ijcr.2006.0168
- Funk, J., Wirth, J., Bonugli, E., & Watson, R. (2012). An Integrated Model of Rolling and Sliding in Rollover Crashes. *SAE International*. doi:10.4271/2012-01-0605
- Gehre, C., Gades, H., & Wernicke, P. (2009). Objective rating of signals using test and simulation responses. *21st International Convergence on the Enhanced Safety of Vehicles (ESV)* (pp. 09-0407). Stuttgart, Germany: NHTSA. Retrieved from <http://www-nrd.nhtsa.dot.gov/pdf/esv/esv21/09-0407.pdf>
- Hanson, R. J., & Norris, M. J. (1981). Analysis of Measurements Based on the Singular Value Decomposition. *Siam J. Sci. Stat. Comput.*, 2(3), 363-373.
- Hovenga, P., Spit, H., Uijldert, M., & Dalenoort, A. (2005). Improved Prediction of Hybrid-III Injury Values Using Advanced Multibody Techniques and Objective Rating. *SAE Technical Paper*, 2005-01-1307. doi:10.4271/2005-01-1307
- Insurance Institute for Highway Safety. (2013, January 13th). *IIHS*. Retrieved from IIHS TechData: <http://techdata.iihs.org/>
- International Organization for Standardization (ISO). (2013). *ISO/TR 16250:2013 Road vehicles -- Objective rating metrics for dynamic systems*. ISO/TC 22/SC 10.
- International Organization for Standardization (ISO). (2014). *ISO/TS 18571:2014 Road vehicles -- Objective rating metric for non-ambiguous signals*. ISO/TC 22/SC 10.
- Jacobs, C., Charras, F., Trosseille, X., Hamon, J., Pajon, M., & J.Y., L. (2000). Mathematical models integral rating. *International Journal of Crashworthiness*, 5(4). doi:10.1533/cras.2000.0152
- Jordan, A., & Bish, J. (2005). Repeatability Testing of a Dynamic Rollover Test Fixture. *19th International Technical Conference on the Enhanced Safety of Vehicles (ESV)* (pp. 05-0362). Washington, D.C.: NHTSA. Retrieved from <http://www-nrd.nhtsa.dot.gov/pdf/esv/esv19/05-0362-O.pdf>
- Kaleto, H., Gatilao, F., & Brumbelow, M. (2010, January 7). *FMVSS 216a and IIHS Roof Crush Webinar*. Retrieved from MGA Research: <http://www.mgaresearch.com/wp-content/uploads/2011/03/RoofCrushWebinar.pdf>
- Kerrigan, J. R., Dennis, N. J., Parent, D. P., Purtsezov, S., Ash, J. H., Crandall, J. R., & Stein, D. (2011). Test system, vehicle and occupant response repeatability evaluation in rollover crash tests: the deceleration rollover sled test. *International Journal of Crashworthiness*, 16(6), 583-605. doi:10.1080/13588265.2011.606996
- Kerrigan, J., Jordan, A., Parent, D., Zhang, Q., Funk, J., Dennis, N., . . . Crandall, J. (2011). Design of a Dynamic Rollover Test System. *SAE International*, 239-271. doi:10.4271/2011-01-1116
- Kerrigan, J., Seppi, J., Lockerby, J., & Foltz, P. (2013). Test Methodology and Initial Results from a Dynamic Rollover Test System. *SAE Technical Paper*, 2013-01-0468. doi:10.4271/2013-01-0468
- Lockerby, J., Kerrigan, J. R., Seppi, J., Foltz, P., & Overby, B. (2013). Optical Measurement of high-rate vehicle roof deformation during rollover. *SAE Technical Paper*, 2013-01-0470. doi:10.4271/2013-01-0470
- MacHey, J. M., & Gauthier, C. L. (1984). Results, analysis and conclusions of NHTSA's 35 MPH frontal crash test repeatability program. *SAE Technical Paper*, 840201. doi:10.4271/840201

- Meyerson, S. L., S., Z. D., & Lund, A. K. (1998). Repeatability of Frontal Offset Crash Tests. *16th International Experimental Vehicle Conference* (pp. 98-S11-O-02). Winsor, Ontario: NHTSA. Retrieved from <http://www-nrd.nhtsa.dot.gov/pdf/esv/esv16/98S11O02.PDF>
- Moffat, E. A., Cooper, E. R., Croteau, J. J., Orlowski, K. F., Marth, D. R., & Carter, J. W. (2003). Matched-pair rollover impacts of rollcaged and production roof cars using the controlled rollover impact system (CRIS). *SAE Technical Paper*, 2003-01-0172. doi:10.4271/2003-01-0172
- Mueller, B. (2013, October 22). Favor: Additional data. Charlottesville, VA, USA.
- Mueller, B. C., Sherwood, C. P., Nolan, J. P., & Zubby, D. S. (2013). Repeatability of IIHS small overlap frontal crash tests. *23rd International Technical Conference on the Enhanced Safety of Vehicles (ESV)* (pp. 13-0079). Seoul, Republic of Korea: NHTSA. Retrieved from <http://www-nrd.nhtsa.dot.gov/pdf/esv/esv23/23ESV-000079.PDF>
- Nash, C., & Paskin, A. (2005). A Study of NASS Rollover Cases and the Implication for Federal Regulation. *19th International Technical Conference on the Enhanced Safety of Vehicles (ESV)* (pp. 05-0415). Washington, D.C.: NHTSA.
- National Highway Traffic Safety Administration (NHTSA). (2009). 49 CFR Parts 571 and 585 Federal Motor Vehicle Safety Standards; Roof Crush Resistance; Phase-In Reporting Requirements; Final Rule. *Federal Register*.
- National Highway Traffic Safety Administration. (2013, January 13th). *NHTSA Vehicle Crash Test Database*. Retrieved from NHTSA: <http://www-nrd.nhtsa.dot.gov/database/veh/veh.htm>
- National Highway Traffic Safety Administration (NHTSA). (2013). *Traffic Safety Facts 2011*. NHTSA. Retrieved from <http://www-nrd.nhtsa.dot.gov/Pubs/811754AR.pdf>
- Nusholtz, G. S., Hsu, T. P., & Byers, L. C. (2007). A proposed side impact ATD biofidelity evaluation scheme using cross-correlation approach. *20th International Conference on the Enhanced Safety of Vehicles (ESV)* (pp. 07-0399). Lyon, France: NHTSA. Retrieved from <http://www-nrd.nhtsa.dot.gov/pdf/esv/esv20/07-0399-O.pdf>
- Office of the Federal Register. (1999). National Highway Traffic Safety Administration –Request For Comments. Docket no. NHTSA-1999-5572; 49 CFR Part 571 – Federal Motor Vehicle Safety Standards; Roof Crush Resistance. *Federal Register*.
- Office of the Federal Register. (2005, August 23). National Highway Traffic Safety Administration –Notice of Proposed Rulemaking. Docket no. NHTSA-2005-22143; 49 CFR Part 571 – Federal Motor Vehicle Safety Standards; Roof Crush Resistance. *Federal Register*, 70(162). Retrieved from <https://www.federalregister.gov/articles/2005/08/23/05-16661/federal-motor-vehicle-safety-standards-roof-crush-resistance>
- Orlowski, K. F., & Bundorf, R. T. (1985). Rollover Crash Tests-The Influence of Roof Strength on Injury Mechanics. *SAE Technical Paper*, 851734. doi:10.4271/851734
- Public Citizen Inc. and Public Citizen Foundation. (2012). *1971 Roof Strength Standard - 33-Year Old Standard Does Not Provide Basic Crashworthiness Protections for Occupants in Vehicles that Rollover*. Retrieved from PublicCitizen: <http://www.citizen.org/documents/The%20Failed%201971%20Roof%20Strength%20Standard.pdf>
- Rossey, M. (2001). Test method for simulating vehicle rollover. *SAE Technical Paper*, 2001-01-0475. doi:10.4271/2001-01-0475
- SAE. (1995, March). J211/1 Instrumentation for Impact Tests .

- Saunders, J., & Parent, D. (2013). Repeatability of a Small Overlap and an Oblique Moving Deformable Barrier Test Procedure. *SAE Int. J. Trans. Safety* 1(2), 2013-01-0762. doi:10.4271/2013-01-0762
- Strashny, A. (2007). *The Role of Vertical Roof Intrusion and Post-Crash Headroom in Predicting Roof contact Injuries to the Head, Neck, or Face During FMVSS No. 216 Rollovers; An Updated Analysis*. Springfield, VA: NHTSA, (DOT HS 810 847) October, 2007.
- Untaroiu, C. D., Shin, J., & Lu, Y. (2013). Assessment of a Dummy Model in Crash Simulations Using Rating Methods. *International Journal of Automotive Technology*, 14(3), 395-405. doi:10.1007/s12239-013-0043-x
- Xu, L., Agaram, V., Rouhana, S., Hultman, R., Kostyniuk, G., McCleary, J., . . . R., S. (2000). Repeatability Evaluation of the Pre-Prototype NHTSA Advanced Dummy Compared to the Hybrid III. *SAE Technical Paper*, 2000-01-0165. doi:10.4271/2000-01-0165